

Review

# A Review on Recent Developments of RCCI Engines Operated with Alternative Fuels

Siva Krishna Reddy Dwarshala <sup>1,\*</sup>, Siva Subramaniam Rajakumar <sup>1</sup>, Obula Reddy Kummitha <sup>2</sup>,  
Elumalai Perumal Venkatesan <sup>3</sup>, Ibham Veza <sup>4</sup> and Olusegun David Samuel <sup>5,6,\*</sup>

<sup>1</sup> School of Mechanical Engineering, SRM Institute of Science and Technology, Kattankulathur, Chennai 603203, Tamil Nadu, India; sr0647@srmist.edu.in

<sup>2</sup> Mechanical Engineering Department, B.V. Raju Institute of Technology, Narsapur 502313, Telangana, India

<sup>3</sup> Department of Mechanical Engineering, Aditya Engineering College, Surampalem 533437, Andhra Pradesh, India; elumalaimech89@gmail.com

<sup>4</sup> Department of Mechanical Engineering, Universiti Teknologi PETRONAS, Bandar Seri Iskandar 32610, Malaysia; ibham.veza@utp.edu.my

<sup>5</sup> Department of Mechanical Engineering, Federal University of Petroleum Resources, P.M.B 1221, Effurun 330102, Nigeria

<sup>6</sup> Department of Mechanical Engineering, University of South Africa, Science Campus, Private Bag X6, Florida 1709, South Africa

\* Correspondence: sivakriv@srmist.edu.in (S.K.R.D.); samuel.david@fupre.edu.ng (O.D.S.)

**Abstract:** Environmental concerns over automotive exhaust emissions and consumer demand for higher fuel efficiency have led to the development of low-temperature combustion concepts. The reactivity-controlled compression ignition (RCCI) engine is one among them and has the potential to reduce NO<sub>x</sub> and smoke emissions simultaneously. In this concept, a low-reactivity fuel is injected into the intake port and another high-reactivity fuel is injected into the cylinder directly. This results in reactivity stratification and provides more control over the rate of heat release. However, operating parameters such as reactivity of fuels, premixing ratio, injection strategies, exhaust gas recirculation ratio, piston bowl geometry, and compression ratio influence emissions formation. The article reviews recent developments on the effect of the above operating parameters on the performance and emission characteristics of RCCI engines operated with alternative fuels. The combustion strategies used to extend the RCCI mode to higher loads are also reviewed. Applications of computational fluid dynamics (CFDs) to design the combustion chamber for RCCI engines are discussed. The need for further improvements in the CFD models for RCCI engines is explained. After presenting a thorough review of recent literature, directions for future research on RCCI engines are proposed.

**Keywords:** low-temperature combustion; reactivity-controlled compression ignition engine; premixing ratio; alternative fuels; emissions



**Citation:** Dwarshala, S.K.R.; Rajakumar, S.S.; Kummitha, O.R.; Venkatesan, E.P.; Veza, I.; Samuel, O.D. A Review on Recent Developments of RCCI Engines Operated with Alternative Fuels. *Energies* **2023**, *16*, 3192. <https://doi.org/10.3390/en16073192>

Academic Editor: Dimitrios C. Rakopoulos

Received: 17 January 2023

Revised: 8 March 2023

Accepted: 26 March 2023

Published: 1 April 2023



**Copyright:** © 2023 by the authors. Licensee MDPI, Basel, Switzerland. This article is an open access article distributed under the terms and conditions of the Creative Commons Attribution (CC BY) license (<https://creativecommons.org/licenses/by/4.0/>).

## 1. Introduction

An internal combustion (IC) engine converts the chemical energy of a fuel into mechanical energy. A wide range of devices such as automobiles, generators, earthmoving equipment, ships, and motorcycles are powered by IC engines. Compression ignition (CI) engines are more efficient in comparison to spark ignition (SI) engines due to their high compression ratio; hence, the IC engine is a preferred choice. However, in the CI engines, it is difficult to achieve a homogeneous air–fuel mixture in the combustion chamber prior to the start of the combustion (SOC) process. This difficulty leads to the development of fuel-rich zones and hotspot regions in the combustion chamber. As a result, NO<sub>x</sub> and soot form in the hot spot and fuel-rich zones, respectively. In addition, incomplete combustion leads to the formation of unburned hydrocarbons (UHCs) and CO (carbon monoxide). These four components, collectively known as automotive exhaust emissions, pollute the environment. Soot causes respiratory diseases [1] and NO<sub>x</sub> results in pulmonary disease [2].

During combustion, the carbon and hydrogen in the fuel are converted into CO<sub>2</sub> (carbon dioxide) and H<sub>2</sub>O (water), respectively. They are expelled into the atmosphere. CO<sub>2</sub> is one of the greenhouse gases and contributes to global warming [3]. To reduce the harmful effect of exhaust emissions on humans and the atmosphere, emission limits are formulated by the government regulatory bodies and these are known as emission standards. Emission regulations put a limit on exhaust emissions.

In Figure 1, it can be seen that from the EU emission standard 1 to EU emission standard 6, the exhaust emission limits are progressively decreased [4]. The original equipment manufacturers (OEMs) should manufacture their engines and cars so that at the tailpipe, the measured emissions should be less than those prescribed by the emission standards. For example, for the Euro 6 standard, tailpipe emissions for NO<sub>x</sub> and smoke should be less than 170 and 5 mg/km, respectively. The exhaust emissions will be measured on the drive cycle that represents highway and city driving patterns. OEMs adopted different technologies to meet emissions standards. Common rail direct injection (CRDI) systems [5] are introduced in place of mechanical injection systems to meet Euro 3 emission limits. CRDI offers great flexibility in optimizing fuel injection timing and quantity. To meet Euro 4 emission limits, an exhaust gas recirculation (EGR) [6] system is used. Split injection strategies [7] were used to reduce combustion noise and emissions. It is not an easy task to meet Euro 4 emission limits. Extensive optimization of valve timings, injection timings, injector flow rate, number of holes in the injector, piston bowl geometry, EGR flow rates, and EGR cooler is required to arrive at optimal trade-off curves for NO<sub>x</sub> and soot limits [8,9]. To meet Euro 5 emission limits, in addition to the above technologies, aftertreatment devices such as catalysts [10] and diesel particulate filters (DPF) [11] are used. The strategy is to use a higher flow rate of EGR to meet the NO<sub>x</sub> through in-cylinder combustion optimization. Higher flow rates of EGR lead to higher amounts of soot, and this is reduced in the DPF.

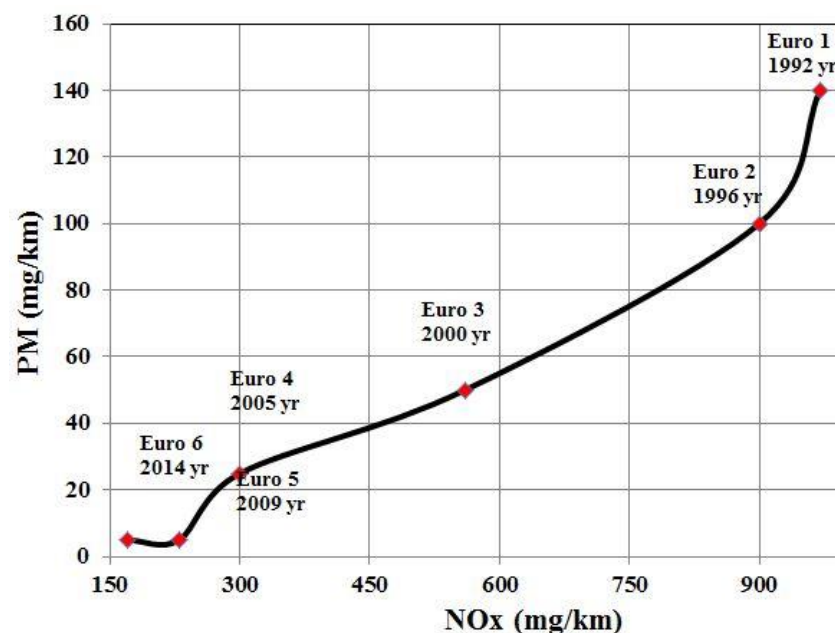


Figure 1. European emission standards for passenger cars [4].

It is very difficult to achieve Euro 6 emission limits by only in-cylinder combustion optimization. Selective catalyst reduction (SCR) [12] technology is adopted to meet NO<sub>x</sub> Euro 6 emission limits. The DPF is used to reduce soot. Both the SCR and DPF are aftertreatment devices, but they increase fuel consumption by offering higher back pressure in the exhaust system. These two aftertreatment devices increase vehicle weight also. A turbocharger is an integral part of a CI/SI engine. This uses exhaust energy, thereby increasing thermal efficiency [13]. A turbocharger sends air at a higher pressure than that

of the atmosphere; hence more oxygen can be accommodated in the given swept volume. Owing to this, additional fuel can be burned, which increases the power output from the engine. As a result, the power density of the engine increases. In addition, the intake port, valve timings, and valve lift are optimized to provide higher volumetric efficiency to the engine [14]. Thus, designing a CI engine is an extremely complicated task. Present state-of-the-art CI engines consist of optimized CRDI, EGR, EGR cooler, catalyst, DPF, SCR, and turbocharger units. There is always an intense effort to develop new technology to reduce emissions and improve thermal efficiency by both academia and industry. One such technique is low-temperature combustion (LTC), which aims to meet the Euro 6 emission limits through in-cylinder combustion optimization, eliminating aftertreatment devices, DPF, and SCR. This offers great flexibility to OEMs in terms of cost and product development time.

There has been significant progress in the development of LTC. In the LTC mode, average combustion temperatures are lower and better homogeneity between air and fuel mixture is achieved. This results in a reduction of the local fuel–air equivalence ratio before SOC. Therefore, it has the potential to lower nitric oxide and soot particles simultaneously. Researchers have developed several LTC approaches [15], such as homogeneous charge compression ignition (HCCI), premixed charge compression ignition (PCCI), and reactivity-controlled compression ignition (RCCI). In the HCCI method, fuel is injected into the combustion chamber during the intake stroke. Because fuel is injected early in the intake stroke, a homogeneous mixture is formed in the HCCI engine. As the fuel–air mixture becomes more homogeneous, it will burn in the premixed phase of combustion [16]. Because of the higher rate of pressure rise and difficulty in controlling the combustion, the operating range of the HCCI mode is limited. These challenges prompted the designers to develop a new concept in LTC strategies, known as PCCI. In this method, control over the combustion is achieved through EGR and early injection of the fuel. Both HCCI and PCCI modes have some shortcomings, such as control of combustion, extending to higher loads, and CO and HC emission control. A new concept, known as RCCI mode [17], was developed for controlling combustion under high-load operation. This method alleviates the disadvantages of HCCI and PCCI modes. In the RCCI mode, Low-Reactivity Fuel (LRF) and High-Reactivity Fuel (HRF) are used to manage the combustion phasing. To improve auto-ignition characteristics, two fuels are combined inside the combustion chamber. Single and multiple injection strategies are used to extend the RCCI concept to high-load operation. In the RCCI engine, the relative benefits of both CI and SI engine operations can be achieved.

The traditional fuels for IC engines are gasoline and diesel. Owing to economic development, sales of IC engines have sharply increased all over the world. As a result, consumption of gasoline and diesel has also significantly increased. For example, in India, petroleum consumption in the second decade of this century increased by 50% compared to the first decade [18]. Petroleum products are derived from fossil fuels, which may get depleted in the future. Further increases in the consumption rate may accelerate the depletion rate. Hence, there is a need to develop new fuels that can substitute gasoline and diesel. To cater to this need, alternative fuels are developed.

Some examples of alternative fuels are alcoholic fuels such as ethanol [19], methanol [20], natural gas [21], and biofuels. The fuels generated from vegetable oils, waste cooking oil, and animal fats are termed as bio-diesel. Ref. [22] investigated ternary fuel by adding bioethanol and rapeseed methyl ester with diesel in the conventional diesel combustion (CDC) mode of operation. Increasing the blending ratio of bioethanol reduced the smoke by 85% at 8 bar IMEP at 2500 RPM. Ref. [23] explored the CDC mode of operation using a ternary fuel by adding methanol and coconut methyl ester with diesel at full load condition of 7 bar BMEP. It was found that increasing the methanol from 10% to 30% improved the brake thermal efficiency by 29% compared to the diesel mode of operation. Smoke opacity was reduced by 38%. Murray and Wyse-Mason [24] investigated various compression ratios (16.5, 15.5, 14.5), variable speed (1500–2500 RPM), and variable load (2–17 bar BMEP) with methane and

diesel as fuel. In the study, CO<sub>2</sub> emissions were reduced by 12% with a compression ratio of 15.5. Ref. [24] explored butanol as ternary fuel with palm oil (20%) +diesel in the CDC mode of operation. The testing was carried out at 3000 RPM under three load conditions of 1.68, 3.37, and 5 bar BMEP. The addition of butanol increased the BSFC by 2% at medium- and full-load conditions. Ref. [25] investigated binary fuel of producer gas using three biodiesels. Rice brain, neem, and honge oil were used to explore the combinations as well as different injection timings and injection pressures in the DI mode. NO<sub>x</sub> (92%) emission was reduced while using binary fuel of honge and producer gas mode at 5 bar BMEP. Ref. [26] developed analytical methods to predict the efficiency of gasoline engines when hydrogen is used as fuel. The chosen engine for this investigation was 8 cylinder, 120 hp at 3200 rpm. From the result, it was found that the specific fuel consumption was reduced by 20%.

Alternative fuels can be extended to LTC concepts also. Many researchers have assessed the performance of HCCI, PCCI, and RCCI engines with alternative fuels. Ref. [27] explored the HCCI operation with port-injected ethanol (3 bars) and intake air temperature ranging from 120 to 150 °C. The temperature was increased to reduce the vaporization time scales in the mixing process. The testing was performed at an IMEP of 4.3 bar, and a thermal efficiency of 44.78% was achieved. Ref. [28] performed a PCCI operation at a load of 4 bars with waste cooking oil (B40) fuel. Thermal efficiency achieved was about 43%. Ref. [29] conducted the RCCI operation by injecting a blend of ethanol (85%) and gasoline (15%) at the port and diesel into the cylinder. The combination of these two fuels resulted in the fuel reactivity stratification and reduced both NO<sub>x</sub> and soot simultaneously. Further, operation with ethanol blend was found to provide a 4% improvement in the indicated thermal efficiency compared to gasoline and diesel RCCI operation at 9 bar IMEP.

There are a few review papers on the details of LTC concepts and biofuels. The work of [30] discusses the origin and combustion characteristics of LTC and its potential to reduce emissions. However, the review article mostly focuses more on the HCCI technology and provides short discussions on RCCI. Similarly, [31,32] presents an extensive review of the effects of fuel properties on engines running with HCCI, PCCI, and RCCI. However, the article does not report much data on the thermal efficiency of LTC engines or a detailed discussion of the operating parameters of RCCI engines. Various EGR configurations and their efficiency in reducing NO<sub>x</sub> emission on both conventional and alternative fuels are explained in [33]. An overview of the various technologies such as biodiesel additives, EGR, emulsion technology, and water injection on CDC operated with biodiesel is given in [34]. A dedicated discussion on the RCCI engine operating with alternative fuels and its potential to reduce NO<sub>x</sub> and soot emissions simultaneously is sparse in the literature. Further, the changes in the thermal efficiency of RCCI engines with respect to CDC engines need to be documented from various sources of literature. The scope of the present work is to provide a comprehensive overview of the RCCI engine operation with alternative fuels and of the effect of its control parameters on emissions and thermal efficiency. The way forward for IC engines, future areas of work in the RCCI operation and advantages of using biodiesel in CDC/RCCI toward CO<sub>2</sub> reduction are discussed.

### 1.1. Basics of CI Engine Operation

Figure 2a depicts the rate of heat release from a CDC engine. The ignition delay period, premixed phase, diffusion phase, and after-burning phase of the combustion are identified. The air–fuel ratio at the periphery of fuel (see Figure 2b) will be within the flammability limits and undergo combustion, releasing heat. This phase of combustion is termed the premixed phase. Peak heat release will occur in this phase. The fuel at the core of the spray will not burn during this phase. As the fuel at the periphery will be consumed by the premixed combustion, the unburned fuel will find its way to the rest of the combustion chamber from the center of the spray. During this transition state, mixing between fuel and air continues and when the air–fuel ratio falls under flammability limits, combustion occurs. This phase represents the diffusion phase and is characterized by a lower heat release rate (HRR), higher crank angle duration, and maximum in-cylinder gas temperature. As the

piston moves downward, the expansion of gases results in a decrease in gas temperature and density. At certain cutoff levels of temperature and density, combustion ceases. The heat released during the ending stage of combustion is termed the after-burning phase.

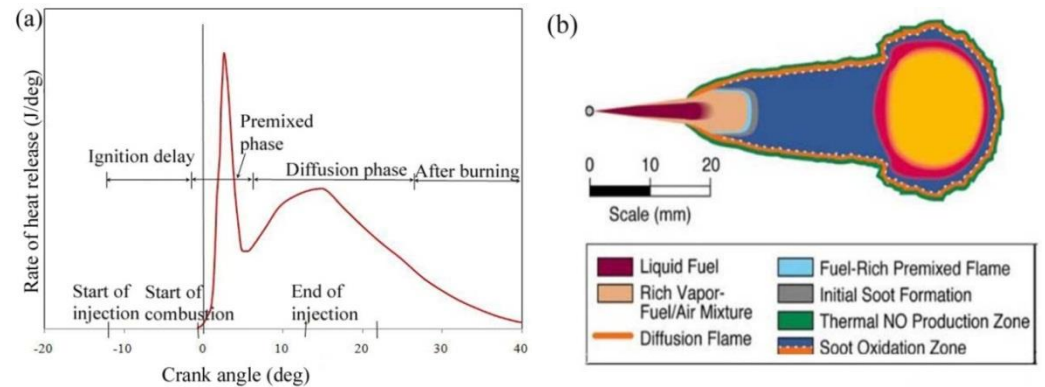


**Figure 2.** (a) HRR curve for a typical CDC engine [35]; (b) depiction of diesel spray in terms of soot concentration contours [36].

Figure 3a shows the mean soot reaction rate for the CDC engine [37]. The crank angles over which positive and negative reaction rates occur overlap with the premixing and diffusion phases of combustion, respectively. Positive and negative signs for reaction rate indicate the formation and destruction of the soot, respectively. Therefore, formation and destruction as well as oxidation of soot occur in the premixing and diffusion phases, respectively. Similar to soot, the majority of NO<sub>x</sub> is formed in the premixing phase of combustion due to higher heat release, i.e., higher in-cylinder gas temperature. To reduce these two emissions, HRR and air–fuel mixing in the premixing phase of combustion need to be controlled. LTC concepts achieve a simultaneous reduction in soot and NO<sub>x</sub> by reducing the fuel–air ratio locally and controlling the HRR in the premixing phase of combustion. The formation of emissions for CDC and LTC concepts as a function of temperature and equivalence ratio is depicted in Figure 3b. Formation of soot occurs when the equivalence ratio is higher than 2. The accumulation of NO<sub>x</sub> occurs when the in-cylinder gas temperature is above 2200 K. The in-cylinder conditions in the CDC model exactly fall in the above range and result in the excessive formation of soot and NO<sub>x</sub>. In the LTC concepts such as HCCI, PCCI, and RCCI, the equivalence ratio and temperature are below 2 and 2200 K, respectively. This paves way for ultra-low NO<sub>x</sub> and soot emissions in the engine exhaust in LTC methods. Comparatively, UHC emissions will be higher in LTC methods due to lower in-cylinder gas temperature.

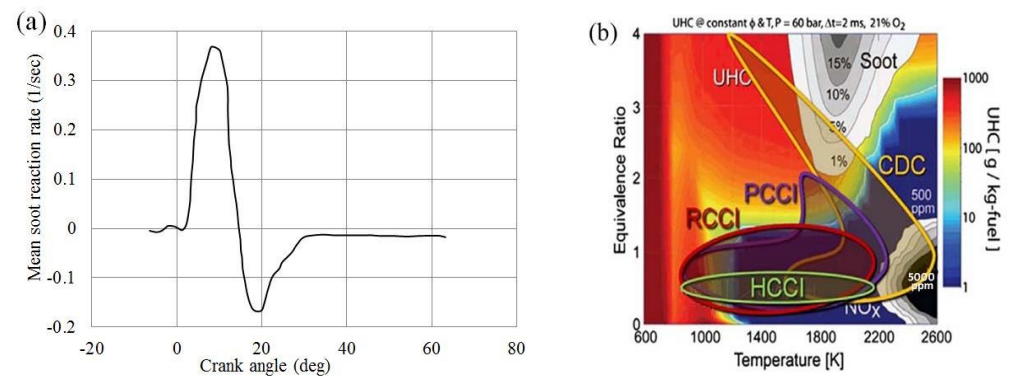


**Figure 3.** (a) Computed mean soot reaction rate in a CDC operation [37], and (b) exhaust emissions as a function of the temperature and equivalence ratio for LTC and CDC concepts [38].

## 1.2. Fundamentals of RCCI

In the RCCI engine, combustion is based on the dual-fuel engine concept. The intake stroke is used to inject LRF into the cylinder (e.g., gasoline, methanol, ethanol, natural gas) so that air and LRF are mixed thoroughly. Towards the end of the compression stroke, HRF is injected into the cylinder under high pressure [38]. The RCCI combustion strategy controls SOC and combustion rate by changing the amount of LRF and the injection timing of HRF. Combustion is improved by higher ignition delay and stratification of fuel charge within the combustion chamber.

### Heat Release

A typical HRR curve of RCCI combustion is shown in Figure 4. The curve has two local maxima with the magnitude of the first one being lower than that of the second one. The first heat pulse is known as low-temperature heat release (LTHR) and the second heat pulse is referred to as high-temperature heat release (HTHR). Usually, the in-cylinder gas mixture temperature in the LTHR phase is lower than that in the HTHR; hence these two regions are termed the low-temperature region (LTR) and high-temperature region (HTR), respectively. The LTR and HTR regions are separated by the negative temperature coefficient (NTC) region. The majority of the fuel burns in the HTHR phase, and the maxima of this phase depend on the amount of LRF.

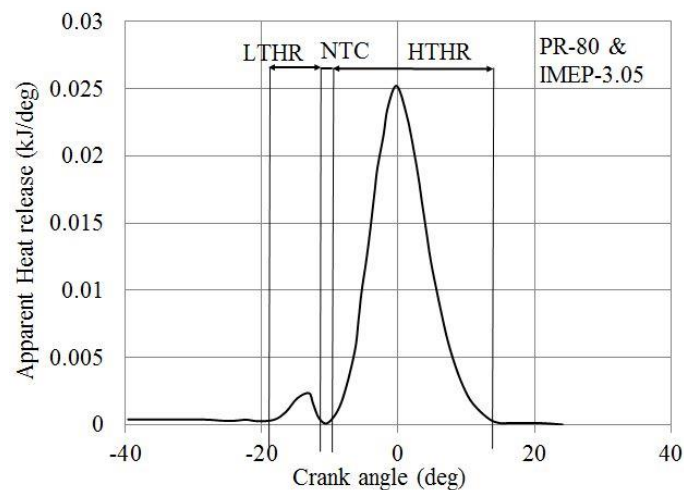


**Figure 4.** A typical HRR curve for an RCCI engine with gasoline/diesel as LRF and HRF, respectively [39].

A comparison between the HRR of CDC and RCCI operations at 5.4 bar IMEP were investigated by Murugan et al. [40]. LRF in these experiments is the mixture of CH<sub>3</sub>OH and polyoxy methylene dimethyl ethers (PODE), and diesel is used as HRF. In the RCCI operation, longer ignition delay (ID) and shorter combustion duration (CD) are observed. Owing to the longer ID, the extent of homogeneity achieved between fuel and air is higher. As a result, soot is reduced by 90%. The diffusion phase is reduced to the minimum level, indicating that before SOC, better homogeneous fuel and air mixture are obtained. The evaporation of LRF, CH<sub>3</sub>OH, is reflected as negative heat release between crank angles (CA) of  $-25^{\circ}$  and  $-13^{\circ}$  (see Figure 3 in [40]). This leads to lower compression pressure and maxima of HRR are also delayed. These two factors reduce the in-cylinder gas temperature and NO<sub>x</sub> formation by 80%. The relative difference in behavior of CDC and RCCI is nearly the same at the chosen engine speeds of 1350, 1600, 1850, and 2100 rpm. The premixing ratio (PR) of the RCCI mode was 77% for all the speeds. The HRR in the RCCI engine is affected by many operating parameters such as type of LRF and HRF, PR of LRF, injection strategies, EGR ratio, piston bowl geometry, and compression ratio. A discussion of these parameters is presented in the following sections.

## 2. Effect of Operating Parameters on Emissions of RCCI Engine

### 2.1. Low-Reactive Fuels

Fuels are divided into LRFs and HRFs based on their properties. Diesel and biodiesel are HRFs based on their high cetane numbers. Increased injection pressure and good atomization of HRF result in less ID and increased in-cylinder pressure in the combustion chamber [38]. Gasoline is considered an LRF based on its high-octane number. In addition to gasoline, alternative fuels such as ethanol, methanol, CNG, NG, biogas, producer gas, acetylene, and isobutyl are considered LRFs. Figure 5a compares the reactivity of diesel, natural gas, and gasoline in terms of ID as a function of temperature [41]. Diesel and NG have, respectively, the lowest and highest ID among these three fuels. The reactivity of fuel can be quantified with ID. Usually, HRF will have a lower ID and LRF will have a higher ID.

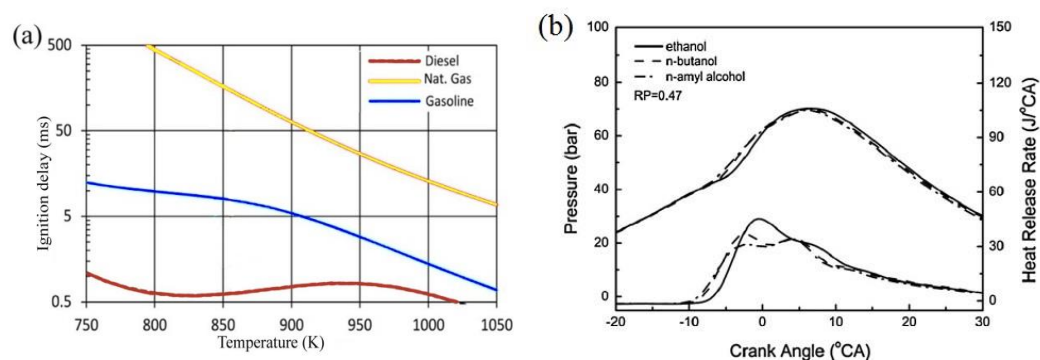


**Figure 5.** (a) Comparison of ignition delay for diesel, natural gas, and gasoline [41]; (b) in-cylinder pressure and HRR with different LRFs [42].

Table 1 lists various fuels that are used as LRF and HRF in RCCI engines and their effect on ignition delay and engine emissions. The “signs +” and “−” indicate an increase and decrease in the respective parameters with reference to the CDC operation. “NA” refers to data not available. A similar notation is used for the tables presented in the rest of the article. The latent heat of vaporization of the fuel is also shown in Table 1. Ethanol has a higher latent heat of vaporization and leads to a higher ignition delay for a given premixing ratio. Figure 5b shows in-cylinder pressure and HRR obtained with ethanol, butanol, and n-amyl alcohol as LRF [42]. PR based on energy is fixed at 0.47 for the three combinations. The three curves deviate from each other in the combustion phase, indicating the effect of fuel properties. The latent heat of vaporization of the ethanol is higher than that of the rest of the two fuels, resulting in higher ID. The combustion duration is also relatively higher. As a result, the in-cylinder pressure obtained with ethanol is lower at the beginning of the combustion and higher in the later stages of the combustion. Similar trends are observed at all the tested PRs of 0.56, 0.65, 0.76, and 0.85. However, the type of fuel has a larger impact on the in-cylinder average temperature. At a PR of 0.45, ethanol yielded a higher  $T_{max}$ , whereas, at a PR of 0.85, n-amyl alcohol has a higher  $T_{max}$ . This resulted in lower  $NO_x$  for ethanol at PR 0.85. The relative difference in PM levels between the fuels is comparatively lower.

**Table 1.** Summary of RCCI engine investigations with different fuels as LRF.

Authors	LRF/HRF	PR %	Latent Heat of Vaporization kJ/kg	ID %	$NO_x$ %	Soot %	HC/CO %
[42]	Ethanol, n-butanol, n-amyl alcohol/diesel	45–85	840, 584, 427	NA	NA	NA	NA
[43]	Ethanol/diesel	0–40	840	30 +	80 −	NA	84/70 +/+
[44]	Isopropanol + butanol + ethanol (3:6:1)/biodiesel	0–66	632	22 +	4.8 −	25 −	96/80 +/+

**Table 1.** *Cont.*

Authors	LRF/HRF	PR %	Latent Heat of Vaporization kJ/kg	ID %	NOx %	Soot %	HC/CO %
[45]	CNG+ H <sub>2</sub> (30%)/sunflower biodiesel	60–80	NA	12+	–	NA	+/+
[46]	Isobutanol/diesel	43–71	578	68+	–	–	+/+
[47]	Methanol/PODE	45–85	630	60+	71–	55–	94/79+ /+

Table 2 illustrates the effect of fuel combinations for LRF and HRF on efficiency and emissions. Iso-butanol has a 23% lesser calorific value and a 14% higher octane number compared to that of gasoline [48]. Higher latent heat of vaporization and octane number of iso-butanol result in longer ID. Due to this, better mixing is achieved and the peak in-cylinder temperature has reduced. Oxygen content in the iso-butanol has accelerated the oxidation process of both HC and CO. Due to these three reasons, the exhaust emissions, NOx, HC and CO were decreased by 5%, 19.7% and 31% respectively with iso-butanol. Altering the HRF from diesel to thevetia peruviana biodiesel has resulted in a decrease in thermal efficiency of 8% [49]. The reduction in NOx emissions is about 5%. HC, CO and soot increased by 21%, 7% and 7% respectively. The poor performance of thevetia peruviana biodiesel is attributed to its higher viscosity and lower calorific value. Effects of PODE as HRF on performance and emissions are investigated by [47]. Compared to diesel, PODE is found to have 1.1% higher thermal efficiency. NOx emissions increased by 44% and those of HC, CO and soot decreased by 38%, 60% and 43% respectively. PODE fuel has less carbon content than diesel which helps to reduce the soot formations.

**Table 2.** Effect of fuel combinations for LRF-HRF on thermal efficiency and emissions at fixed engine speed of 1500 RPM.

Authors	LRF	HRF	PR %	Operating Conditions	BTE/ITE	NOx	HC	CO	Soot
[48]	Gasoline	Diesel	40–60%	2.4 bar IMEP, IP-800 bar	–	4	13.7	67.5	–
	Iso-butanol	Diesel	40–60%	2.9 bar IMEP, IP-800 bar	–	3.8	11	46	–
[49]	Gasoline	Diesel	10–50%	3.14 bar BMEP, IP-900 bar	23	2.7	0.9	0.72	4.1
	Gasoline	Thevetia peruviana biodiesel	10–50%	3.14 bar BMEP, IP-900 bar, B20	21	2.55	1.15	0.78	4.4
[47]	Methanol	Diesel	70–85%	3.4 BMEP, IP-480 bar, EGR 26	30.75	1.2	2.6	4.5	0.016
	Methanol	PODE	70–85%	3.4 BMEP, IP-480 bar, EGR-26	31.1	2.15	1.6	1.8	0.009

## 2.2. Premixing Ratio

The ratio of the mass of LRF to the summation mass of LRF and HRF is known as the premixed ratio. PR is one of the dominant parameters that affect the performance and emissions of RCCI engines. [47] conducted experiments on the CDC and RCCI modes at a speed of 1500 rpm. Diesel and PODE were used as HRF. CH<sub>3</sub>OH was used as an LRF and PRs used were 70, 75, 80, and 85 with an injection pressure of 3 bar. For all these trials, the EGR rate was fixed at 26%. Figure 6a shows pressure and HRR obtained with PODE as HRF at 3.4 bar BMEP. The solid line represents CDC operation with PODE as fuel. The compression pressure is higher with CDC operation. With the introduction of LRF in the RCCI operation, compression pressure reduces. This is due to the vaporization of LRF. With the increase in PR, the amount of heat taken by LRF for vaporization from the in-cylinder

gas mixture increases. As a result, the compression pressure and temperature decrease as the PR increases. This also leads to an increase in the ID with an increase in the PR. The maxima of HRR increase as the PR is increased. However, the crank angle at which maxima occur shifts away from the top dead center (TDC), leading to lower in-cylinder gas temperatures.

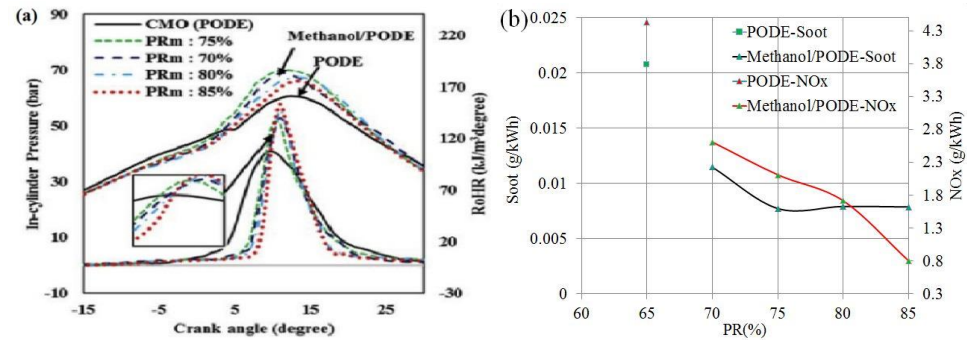


**Figure 6.** Effect of premixing ratios. (a) In-cylinder pressure and HRR, and (b) emissions as HRF at 3.4 bar BMEP and speed 1500 RPM [47].

Figure 6b shows that NO<sub>x</sub> decreases as the PR increases from 70 to 85. This is due to the reduction in the average gas temperature, with the increase in PR. At this load point, it is observed that soot is not a strong function of PR. HC and CO emissions are found to increase with the increase in PR. Testing was done with diesel as HRF also. It was observed that HRR and in-cylinder pressure obtained with diesel were lower than those of PODE. Unstable engine operation was noticed when PR was more than 85%.

A similar investigation was performed by [44] at 2400 RPM on a single-cylinder engine. A mixture of isopropanol, butanol, and ethanol with a volumetric ratio of 3:6:1 was used as the LRF and diesel and biodiesel were used as the HRFs. The injection pressure of HRF was about 300 bar and that of LRF was about 5 bar. Engine performance and emission data were measured for PRs of 0, 15, 30, 45, and 60 and corresponding HRR for a load of 15.42 Nm, and are shown in Figure 7a. With the increase in PR, the in-cylinder pressure and HRR also increase. Owing to the vaporization of the LRF, as the PR increases, pressure and temperature toward the end of compression decrease. This increases the extent of mixing and ID, and the majority of the LRF burns in the premixing phase. As a result, the HRR and in-cylinder pressure and rate of pressure rise increase as the PR increases. This effect is more pronounced as the load on the engine is increased (see Figure 7b). For the 60% load condition, when the PR is increased from 15 to 60, NO<sub>x</sub> increased by 43% and smoke decreased by 93%. However, both HC and CO increased by 75% and 9.6%, respectively. Table 3 provides a summary of recent investigations on RCCI engines with different PRs keeping ethanol as the LRF. Corresponding HRF, load point, injection timings, and emissions are also given. The “signs” “+” and “−” represent relative change with respect to minimum PR. The same convention is used in the rest of the tables.

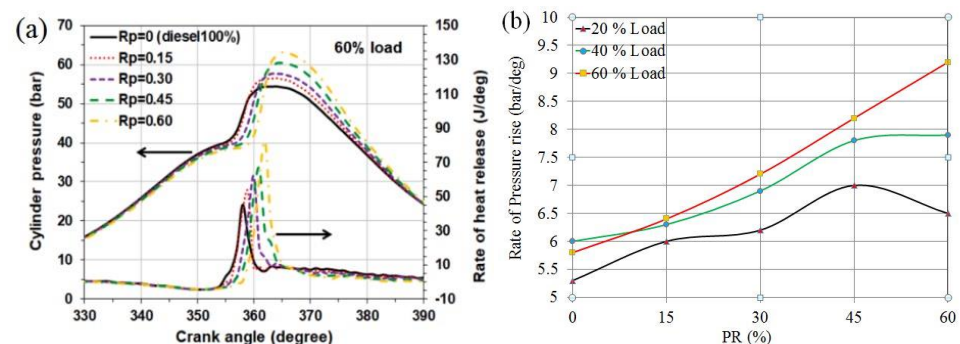


**Figure 7.** Influence of PR on RCCI operation. (a) In-cylinder pressure and HRR, and (b) ROPR [44].

**Table 3.** Summary of studies on RCCI engines with different premixing ratios keeping ethanol as LRF.

Authors	HRF	PR %	BMEP (Bar)/CR	Injection Timing (bTDC)	NOx %	Soot %	HC/CO %
[42]	Diesel	47, 57, & 67	6.1/18.5	60 & 30	—	+	+/+
[50]	Diesel	60 & 80	9.6/16	14–11	—	—	+/+
[51]	Mahua biodiesel	10–90	6.3/17.5	55–23	—	—	+/NA
[52]	Safflower Biodiesel	30 & 50	7.6/17	15	50 —	NA	76/25 +/+

### 2.3. EGR Rate

Under high load conditions, excessive pressure rise is observed in the RCCI mode [53]. The EGR technique can be used to control the rate of pressure rise [54]. Owing to its higher heat capacity and by reducing oxygen availability, EGR controls the rate of pressure rise. It also results in a reduction of NO<sub>x</sub>, similar to that observed in the CDC operation. However, EGR is bound to reduce thermal efficiency and increase HC and CO emissions. Hence, a trade-off study between emissions, rate of pressure rise and efficiency needs to be conducted. [55] investigated the effect of EGR on the rate of pressure rise and emissions on a four-cylinder turbocharged engine at IMEP of 8 bar and speed of 2000 RPM with a swept volume of 1.6 L. The LRF and HRF are methane-rich natural gas and hydro-treated vegetable oil, respectively. High PR ranging from 57% to 94%, which represents high load operations, is used. Figure 8a shows the effect of EGR on the rate of heat release for PR of 88%. EGR strongly suppresses premixed combustion and increases the CD. Heat release curves shift away from TDC, indicating the reduction in the rate of pressure rise. As the EGR increased from 0% to 8%, 15%, and 23%, the peak HRR decreased by 32%, 36%, 42%, and 59%, respectively, compared to that of the non-EGR cases.

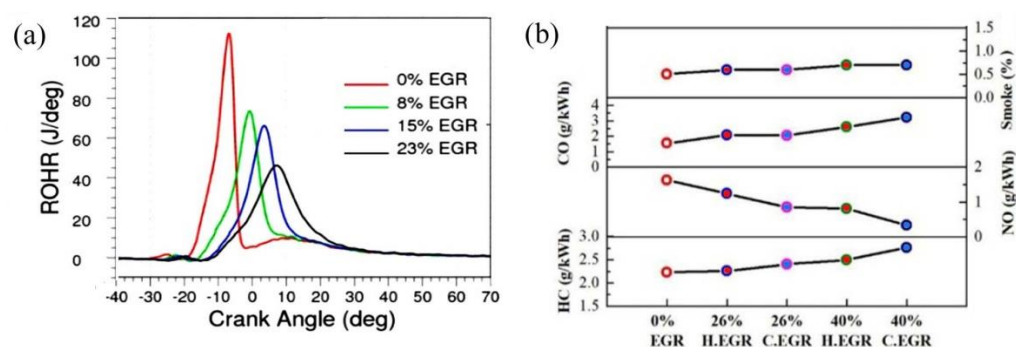


**Figure 8.** Effect of EGR rate on RCCI operation. (a) ROHR at BMEP of 8 bar [55], and (b) Emissions at BMEP of 5.1 bar [56].

For the same load point, the authors explored different combinations of PRs and EGR ratios and their effect on NO<sub>x</sub> (see Figure 9a). For a given EGR rate, as the PR in terms of the energy share increases, NO<sub>x</sub> reduces. This is mainly due to the cooling effect of LRF. Figure 9a also indicates that a higher amount of EGR is required to control the NO<sub>x</sub> emissions for lower PRs. For a given EGR rate, soot decreases as the PR increases (see Figure 9b). As PR is increased, more amount fuel burns in the homogeneous phase, thus resulting in the reduction of soot. A combination of lower PR and higher EGR rate leads to higher soot formation. The influence of cold EGR on emissions is shown in Figure 8b for BMEP of 5.1 bar [56]. On X-axis, “H.EGR” and “C.EGR” represent hot and cold EGR respectively. Cold EGR reduces the NO<sub>x</sub> further compared to hot EGR, and accordingly, a lower rate of pressure rise is also observed. However, it has a significant adverse effect on HC and CO emissions and a marginal effect on smoke.

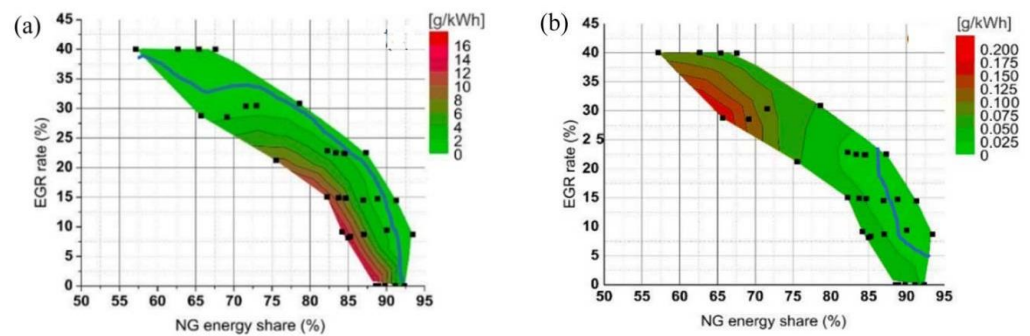


**Figure 9.** Contour map of (a) NO<sub>x</sub>, and (b) soot as a function of the premixing ratio and EGR rate at load point of 8 bar BMEP and 2000 rpm [55].

The effect of the temperature of the mixture under intake valve close (IVC) conditions on HRR and emissions was investigated numerically by [57]. AVL FIRE along with Chemkin II was used to simulate RCCI combustion and to predict engine-out emissions. Load conditions were 4 bar IMEP and 800 RPM. Except for the 5% EGR, HRR continuously decreased with an increase in the EGR rate, as shown in Figure 10a. A similar effect on LTHR also can be noticed. Note that, in simulations, the angle at which peak in HRR occurs is not strongly influenced by EGR, opposite to that observed in test data, as shown in Figure 8a. As the temperature of the mixture at IVC is increased (see Figure 10b), autoignition of the mixture occurs earlier and higher HRR can be noticed. This leads to higher peak firing pressure. [58] Investigated the performance of the RCCI engine at 1500 RPM with natural gas and diesel as LRF and HRF respectively, PR 80%. Effects of variations in injection pressure (300–2400 bars), EGR (0–36%), and SOI (8–30% CA bTDC) on performance and emission were studied using an experimental and computational approach. The findings showed that with the introduction of 33% EGR, NO<sub>x</sub> reduces by 68%. Some of the other recent investigations with EGR using different alternative fuels are shown in Table 4. The attempted LRFs are natural gas, gasoline, butanol, and iso-butanol. The PRs are in the range of 35–80 and the EGR rate is in the range of 15–50. In all these investigations, with the EGR, NO<sub>x</sub> was reduced with a penalty on HC/CO emissions. The highest reduction was achieved in NO<sub>x</sub> and soot (with respect to PR) for the combination of iso-butanol and diesel for a load of 2.7 bar, with an EGR ratio of 22 [46]. Note that for this combination, there was a drastic reduction in NO<sub>x</sub> and soot emissions simultaneously, which is required for Euro 6/BS 6 emission regulations.

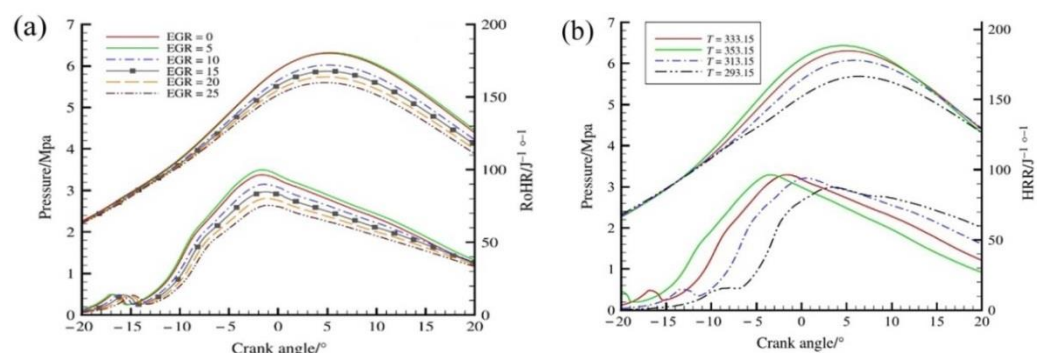


**Figure 10.** Effect of (a) EGR rate, and (b) mixture temperature at IVC on HRR and in-cylinder pressure for an RCCI engine [57].

**Table 4.** Summary of RCCI investigations with different EGR rates and their influence on engine emissions.

Authors	LRF/HRF	IMEP Bar	PR%	EGR%	NO <sub>x</sub> %	Soot%	HC/CO%
[46]	Iso-butanol/diesel	2.7	43–71	22	–	–	+/+
[54]	Butanol/biodiesel	4–12	60–80	20–47	–	+	+/+
[56]	Methanol/diesel	3.4 & 5.1	57–90	0–40	–	–	+/+
[59]	E20-95/B7	7.5	49–79	41–53	–	NA	+/-
[60]	Natural gas/diesel	4–6	55–95	15, 20	–	NA	+/+
[61]	Natural gas/diesel	4, 9, 23	35	0–48	–	+	+/+

#### 2.4. Compression Ratio

Compression ratio (CR) is one of the design parameters that influence performance and emissions significantly. The higher the CR, the higher the compression pressure, temperature, and density. These three factors reduce the ID as well as mixing delay. As a result, the combustion rate and indicated thermal efficiency will be higher at higher CRs. However, higher temperatures result in higher engine-out NO<sub>x</sub> emissions. Therefore, CR is preferred to reduce NO<sub>x</sub> emissions with a penalty on efficiency and HC/CO emissions. A similar logic extends to RCCI engines also. The HRRs for CRs of 17 and 14 at 10 bar BMEP are shown in Figure 11a. The LRF and HRF are CNG and diesel, respectively [62]. Higher ID, lower peak HRR, and higher CD can be noticed for CR 14. Further LTHR is not clearly visible. Toward the end of the expansion, CR 14 has a higher temperature, and hence lower CRs will have higher expansion temperatures compared to those with higher CRs. The effect of CR on emissions is shown in Figure 11b.

CR 14 emits 10%, 71%, and 64% lower NO<sub>x</sub> emissions compared to CR 17 for engine speeds of 1200, 1500, and 1800 rpm, respectively. HC emissions are higher by about 35% at all speeds. Non-monotonic changes in the soot and CO emissions are noticed. This indicates that soot is mostly influenced by local thermodynamic conditions rather than average gas conditions. [63] investigated CR effects on an RCCI engine numerically. Closed cycle combustion simulations were performed for CRs of 12, 13, 14, 15, 16.1, and 17. By changing the position of the cylinder head, the CR of the engine was changed. LRF and HRF used in the simulations were gasoline and diesel, respectively. Figure 12a shows HRR obtained with CRs of 12, 14, and 16.1. With the decrease in CR, a decrease in the rate of pressure rise and HRR was noticed. Another method to reduce CR is to delay IVC timings. Using this approach, the authors studied the RCCI performance for identical CRs. The obtained HRR values for lower CRs are similar to those presented in Figure 12a. Engine-out emissions obtained with different CRs are shown in Figure 12b. Low CR meets Euro 6 limits of NO<sub>x</sub> and soot with good tolerance. Table 5 summarizes recent works on different CRs with RCCI engines. The minimum CR attempted is 11, and in the study [62], the maximum load operated with a CR of 11 was 21 bar. Under this load condition, the exhaust emissions were within Euro 6 limits.

**Table 5.** Summary of RCCI engine investigations with different compression ratios and their effect on engine emissions.

Authors	LRF/HRF	CR	PR%/EGR%	IMEP Bar	NO <sub>x</sub> %	Soot%	HC/CO%
[64]	Biomass/diesel	12–18	34–48/NA	3.17, 4.23	NA	NA	+/+
[62]	CNG/diesel	14 & 17	63.4–88.9/42, 51	7, 9, 10	–	–	+/+
[65]	Gasoline/diesel	14.4 & 11	75 & 80–70/NA	6.9 & 14–23	–	–	+/+

Table 5. Cont.

Authors	LRF/HRF	CR	PR%/EGR%	IMEP Bar	NO <sub>x</sub> %	Soot %	HC/CO %
[66]	CO <sub>2</sub> /diesel	20	25–45/NA	6.5	44 +	10 +	18/6 +/+
[67]	CNG/safflower biodiesel	13–19	5–15/NA	17.34	50 –	39 –	1/4 +/+

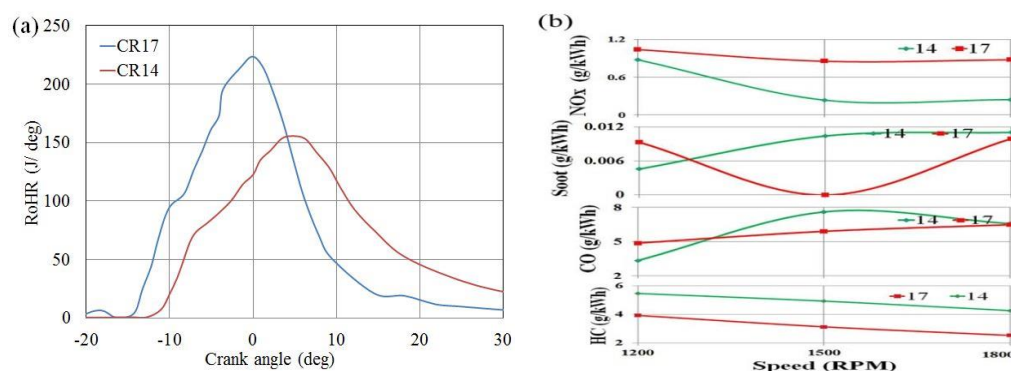
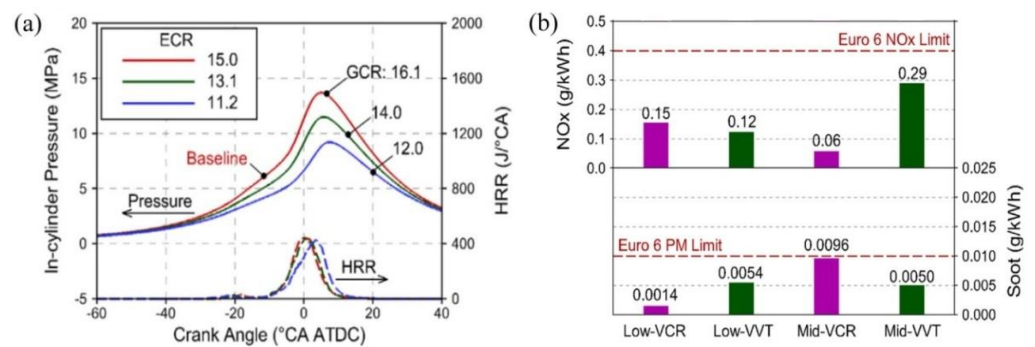


Figure 11. Effect of compression ratio on (a) HRR, and (b) emission in the RCCI mode of operation [62].

### 2.5. Bowl Geometry

The in-cylinder phenomena such as fuel–air mixing, swirl and tumble motion of fuel–air mixture, amplification of turbulence, and swirl during the compression process are strongly influenced by the piston bowl [37]. Hence, the shape of the piston bowl needs to be optimized to reduce emissions and fuel consumption. In the RCCI mode, fuel injections will be very much advanced or delayed. A further amount of HRF that needs to be injected for a given load point will be lower compared to that of the CDC. Therefore, injection duration will be lower, and accordingly, the piston bowl shape needs to be redesigned for optimum performance of the RCCI engine.

Performance and engine-out emissions of RCCI engines were investigated with three-piston bowls at 1200 RPM and are shown in Figure 13a [65]. The base piston bowl is stock, and the other two are modified in the squish region to reduce HC and CO emissions. The modified piston bowls also have a lower surface area and hence reduce heat transfer losses during the combustion. The piston bowls have a compression ratio of 14.4 and are tested at low, medium, and high load points. From the experimental data, it is observed that the RCCI combustion is sensitive to the piston bowls at low load points. At medium- and high-load points, the extent of sensitivity is lower. Figure 13b shows emissions at a high load point at 19.3 bar IMEP with the three-piston bowls. Combustion is optimized with both single- and double-injection strategies. Excessive soot levels are noticed with the double-injection method whereas, with single-injection, engine-out soot levels are within Euro 6 emission limits. Among the three-piston bowls, soot levels obtained with the bathtub piston bowl are higher. The corresponding heat release curves and mean gas temperatures are shown in Figure 14. The combustion is characterized by four peaks in the HRR. The bathtub piston bowl with a single injection has a lower magnitude in the HTHR region, which caused higher soot levels. Extensive combustion optimization is performed at all three load points, and using optimization techniques, it was found that the most suitable bowl geometry for the RCCI operation is stepped geometry.



**Figure 12.** Comparison of (a) in-cylinder pressure and HRR, and (b) emissions obtained on a RCCI engine with different CRs [67].

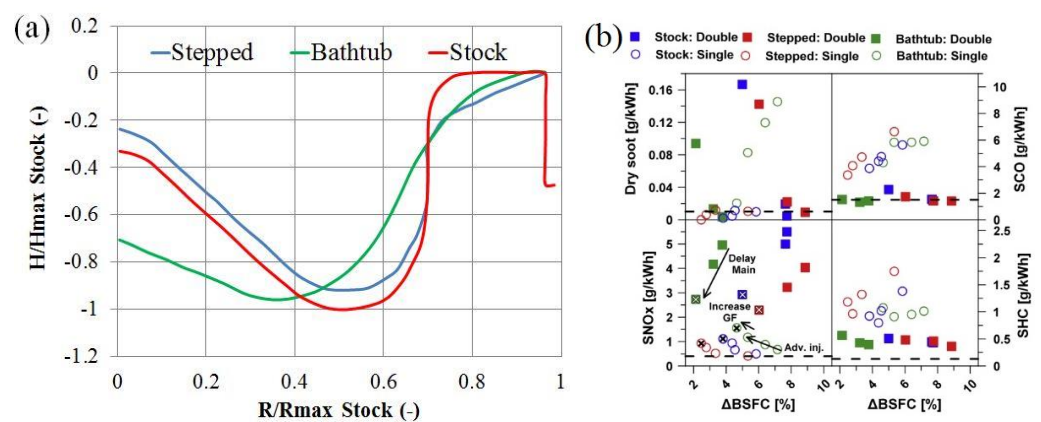


**Figure 13.** Effect of piston bowl shape on the RCCI operation at 1200 rpm and high load point. (a) Geometric shape, and (b) emissions obtained with single and double injections [65].

To quantify the effects of change in piston bowl geometry on heat transfer losses, computational fluid dynamics (CFD) simulations were performed on the above three bowls, that is, stock, stepped, and bathtub by [68]. The conditions in CFD simulations were identical to those of testing given in reference [65]. The CFD-predicted HRR, HC, and CO emissions were compared with those of the testing data. LTHR was captured by predictions. However, at a high load point, significant deviations between predicted and measured emissions were noticed, and the deviation was highest for the bathtub piston bowl. The CFD solution data analyzed and heat transfer losses for the three bowls are represented in terms of a bar chart. Figure 15a,b represents the budget of fuel energy for the three bowls for low and high load points. The bathtub piston has a 16% lower surface area, and this resulted in reducing the heat transfer losses by 7.89% at a low load operating point. However, such high benefits are not realized at high-load operating points. On the basis of the gross indicated work, authors chose the stepped piston bowl, which has a medium reduction in surface area, as the optimum combustion bowl for RCCI engines that can operate from low to high load operating points.

The effects of shape and depth of the piston bowl and chamfered ring-land on the performance and emissions of RCCI engines were investigated numerically by [61]. The chosen piston bowl shapes were stock, bathtub, and cylindrical, which are shown in Figure 16a. Converge software was used for simulations, and chosen engine speeds were 800, 1300, and 1800 RPM. The LRF and HRF are natural gas and diesel, respectively. The piston bowl profiles have a large impact on NOx formation with the bathtub bowl producing the highest NOx at the three chosen engine speeds. As the surface area is lower for the bathtub profile, it has relatively higher gas temperatures, as shown in Figure 16b, and leads to higher NOx emissions. When bowl depth changes, it alters the piston surface area and squish area. These two factors change heat transfer losses and mixing between air

and HRF. Enhancing bowl depth increases piston surface area, hence more heat losses; on the other hand, it improves the mixing process and leads to improvement in combustion. These two factors counter each other to give net benefits. A bowl depth of 1 cm was found to be optimum for the chosen engine conditions. Similar trends were observed with the chamfering radius of the ring-land. Other notable works on the design of piston bowls for RCCI engines include [69–71]. The main idea in these works was to reduce the HC/CO emissions by optimizing the bowl depth and squish region.

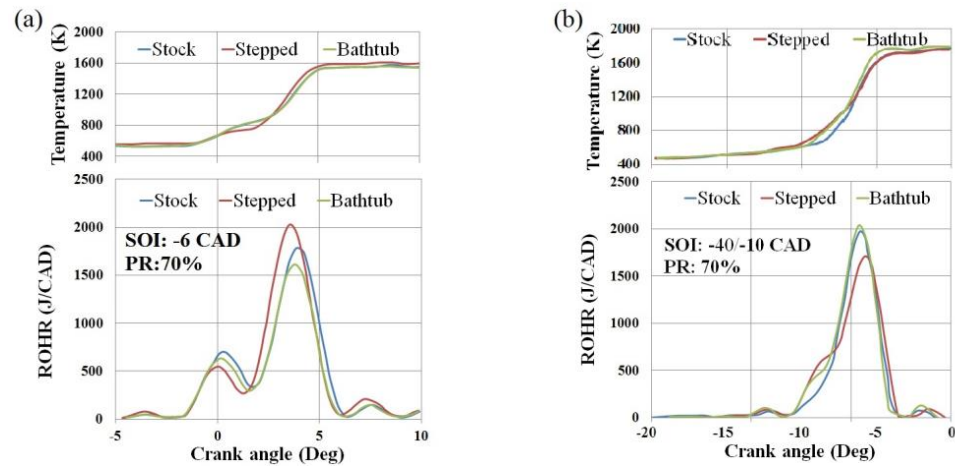


Figure 14. HRR curves obtained with (a) single and (b) double injections at high load point with the three–piston bowls [65].

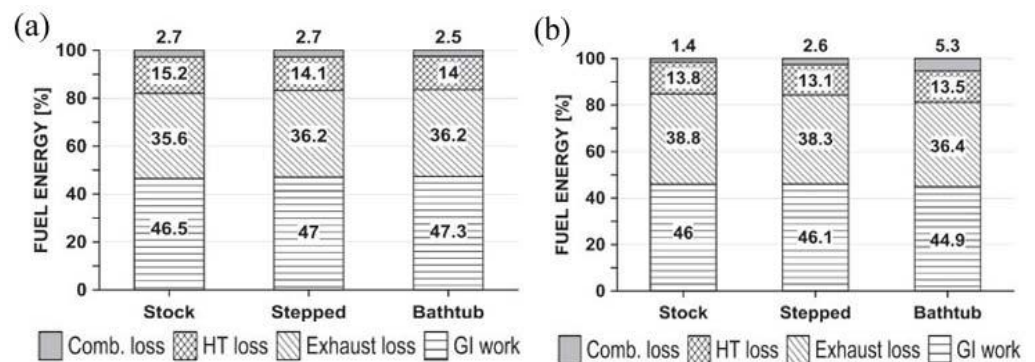


Figure 15. Budget of the fuel energy predicted from combustion simulations for different bowls at (a) low load and (b) high load operating points [68].

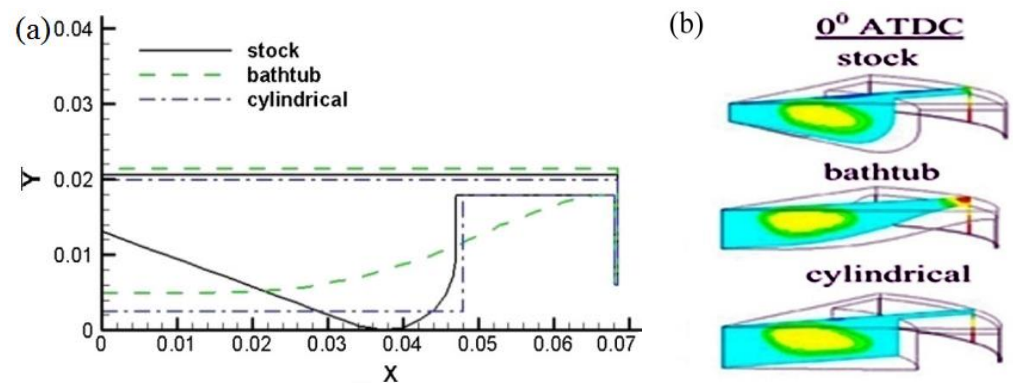
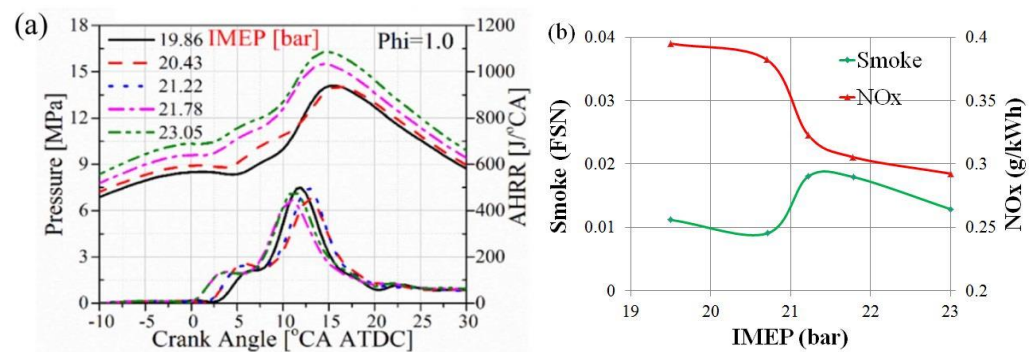


Figure 16. Comparison of (a) shape of the piston bowls, and (b) temperature distribution obtained from Converge software at 9 bar IMEP and speed of 800 rpm [61].

## 2.6. High Load Operation of RCCI

As the load on the engine increases, the fuel quantity that is injected into the engine needs to be increased. This leads to the enhancement of PR. As a result, the majority of the fuel burns in the premixing phase. Hence, an excessive rate of pressure rise and autoignition of the fuel and air mixture occurs [72]. Therefore, control of pressure rise at high load operation is required for the successful implementation of RCCI on production vehicles. Pressure rise can be countered by reducing the compression ratio, incorporating EGR, and adopting innovative injection strategies. In the RCCI mode, a six-cylinder turbocharged engine at high loads was tested [73]. LRF as gasoline and HRF as PODE were used to achieve RCCI operation. The IMEP values of load point are 19.86, 20.43, 21.78, and 23.05 bars. The corresponding cylinder pressure traces and HRRs are shown in Figure 17a. The EGR technique along with a late injection of HRF (3–9° before TDC) was used to control the pressure rise. The amounts of EGR and injection timings were controlled so that the maximum pressure rise was below 12 bar/CA. Owing to late injection, combustion of premixing fuel occurs after TDC. The amounts of EGR used for the above load conditions were 28.8, 32.4, 33.7, 34.5, and 35.9 respectively. Engine-out emissions are shown in Figure 17b. There is a continuous reduction in NO<sub>x</sub> as the load increases. This is due to an increase in the EGR rate with respect to load. Smoke initially increases and then decreases. The investigation shows that EGR and late injection can achieve high-load operation.



**Figure 17.** Operation of RCCI engine at high load operating points: (a) HRR and in-cylinder pressure curves, and (b) emissions, NO<sub>x</sub>, and smoke [73].

Ref. [74] achieved high loads with the combination of EGR and low compression ratio. LRF and HRF used in this study were gasoline and diesel, respectively, and PR for all the high load points was in the range of 30–50%. Single- and late-injection strategies were used for combustion. Figure 18a shows the EGR map used on a 15.3 compression ratio engine. For high loads, i.e., IMEP > 15 bar, the EGR rate is in the range of 45 to 30%. The percentage of difference in NO<sub>x</sub> emission between CDC and RCCI for the above engine is shown in Figure 18b. It can be inferred that at a load of 1500 RPM, and 23 bar, RCCI operation results in a reduction of NO<sub>x</sub> by 95% compared to that of CDC.

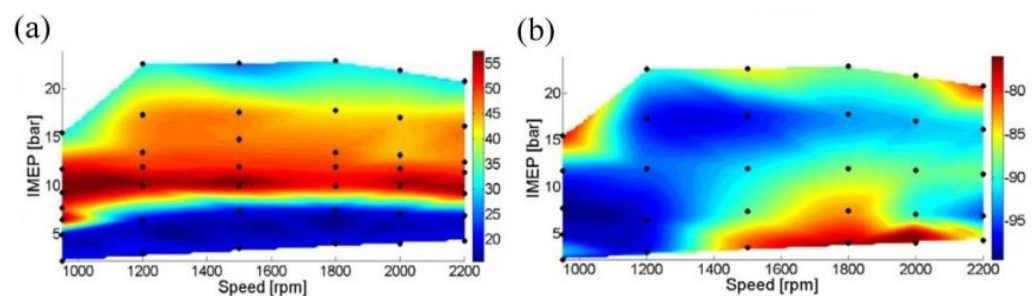


**Figure 18.** Percentage difference between emissions obtained on RCCI and CDC engine as a function of speed and IMEP. (a) EGR, and (b) NO<sub>x</sub> [74].

The possibility of achieving high loads with a split-injection strategy was investigated numerically by [41]. CR of 16.1 and EGR were used to control the combustion rate with split injection. The HRF and LRF were diesel and gasoline, respectively. Figure 19a shows cylinder pressure traces and Figure 19b shows HRR for IMEP of 13.5, 16, and 23 bar. SOI1 and SOI2 for 23 bar load points are 92.7 and 20.4 bTDC, and corresponding mass ratios are 70% and 30%, respectively. For all the high load points considered in this work, the rate of pressure rise was below 8 bar/deg. Table 6 lists high-load operations achieved by other authors. In the majority of the trials, gasoline is used as LRF. PR is in the range of 50–90%. The EGR rate is in the range of 40–60%. Simultaneous reduction of NO<sub>x</sub> and soot was achieved with the RCCI operation at high load operation. Compared to low-load operating points, enhancement in HC/CO emissions is relatively higher. The rate of pressure rise is between 8 and 12 bar/deg.

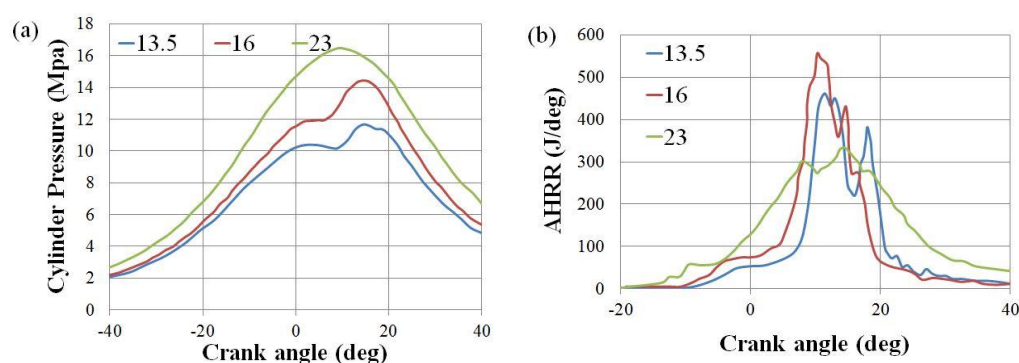


**Figure 19.** Effect of load on the RCCI engine operated with split-injection strategy: (a) in-cylinder pressure, and (b) HRR [41].

**Table 6.** Summary of investigations performed on RCCI engines at high load operating points.

Authors	LRF	HRF	PR%/EGR%	IMEP Bar	ROPR (Bar/Deg)	NO <sub>x</sub> %	Soot %	HC/CO %
[29]	E85	Diesel	83/47	16.5	10	—	—	—
[70]	Ethanol	Diesel	85/40	17	10	NA	NA	—/—
[73]	Gasoline	PODE	70/42, 65	13.5	12	—	—	NA/NA
[74]	Gasoline	Diesel	0–80/NA	20	15	85	NC ↔	NA/NA
[75]	Gasoline	<i>n</i> -Heptane	89/41	14.6	—	—	—	NA/NA

↔ No Change, NA—Not Available.

### 3. Discussion and Directions for Future Research

Brake thermal efficiency obtained with CDC and RCCI operations is listed in Table 7. Other conditions such as compression ratio, load, speed, fuel, % change in NO<sub>x</sub>, and smoke emissions are also shown in the table. In CDC with a compression ratio of about 17.5, at loads of 4.5–6 bar, brake thermal efficiency ranges from 34% to 38%. Depending on the operating conditions, the usage of biodiesel can result in a reduction of brake thermal efficiency by about 5% compared to that obtained with diesel. The change in thermal efficiency is contributed by multiple factors such as viscosity, calorific value, flash point, and the presence of oxygen atoms in the fuel. Factors such as high viscosity and lower calorific value result in a decrease in thermal efficiency. On the other hand, oxygen atoms accelerate the combustion process, leading to improvements in thermal efficiency. These two factors counter with each other to give a net reduction of about 5%. Owing to its higher oxygen content, biodiesels emit a lesser amount of CO and HO compared to diesel. With the RCCI cycle, brake thermal efficiency ranges between 45% and 55% depending on the type of fuel and other operating conditions. RCCI improves thermal efficiency by reducing

exhaust and heat transfer losses. Lower HRRs reduce heat transfer losses, and lower in-cylinder temperature reduces exhaust losses. The highest thermal efficiency achieved, was about 60% with the RCCI cycle (see Table 7, row 6). The highest efficiency was achieved by piston cooling, modified piston bowl geometry, reduction of pumping losses, reduction of thermal losses, etc. There was nearly a 5–10% increase in thermal efficiency when engine operation switched to RCCI from CDC. The improvement in thermal efficiency results in a reduction of CO<sub>2</sub> emissions. Therefore, choosing the RCCI cycle over CDC will directly yield 5–10% lower CO<sub>2</sub> emissions. Additionally, RCCI results in a reduction of both NO<sub>x</sub> and soot emissions.

Extensive research has been conducted on RCCI engines to understand various factors that influence engine operation, and RCCI engines have the capacity to meet Euro 6 emission standards without aftertreatment devices. To take this technology to production engines, more investigations need to be performed. Blends of hydrogen- and alcohol-based biofuels can be used as LRF. Hydrogen has the potential to reduce HC and CO emissions due to its fast-burning rate. Adding hydrogen reduces net hydrocarbon fuel, thereby reducing CO<sub>2</sub> emissions. Systematic optimization of the LRF injector location can be performed by using a computational approach. Injector properties such as nozzle hole diameter, pulse rate, and injection pressure can be optimized. Mixing between air and LRF, air + LRF mixture, and HRF can be improved by optimizing the swirl ratio of the intake port.

Choosing the appropriate combination of LRF and HRF is required for improving efficiency and reducing emissions simultaneously. A combination of iso-butanol and diesel was found to outperform the gasoline-diesel combination. Gasoline- thevetia peruviana biodiesel has resulted in 8% lower thermal efficiency compared to gasoline-diesel combinations. So further research is required to compensate for the reduction in thermal efficiency. The methanol-PODE combination was found to have higher NO<sub>x</sub> by 44% compared to the methanol-diesel combination with 1.1% higher thermal efficiency. Enhancement in NO<sub>x</sub> with a corresponding reduction in soot may not bring the trade-off curve closer to emission regulation margin limits. Even though the combination results in LTC, the simultaneous reduction in NO<sub>x</sub> and soot has not occurred. Hence further research is required to improve the emission aspects. As fuel stratification is dominant in RCCI combustion, a proper combination of HRF and LRF is required to take the benefits of the LTC behavior. Hence investigations should be performed to determine the correct combinations of fuels for LRF and HRF.

**Table 7.** Comparison of brake thermal efficiency obtained under CDC and RCCI conditions with alternative fuels.

Reference	Operated Conditions	Fuel	Performance		Combustion	Emissions	
			A-BTE	D-BTE %		NOx %	Smoke %
[76]	CR of 17.5 in CDC mode at 6 bar with 1500 rpm	Corn oil (B10)	34.5	1.27 ↓	Negligible change in pressure and heat release compared to diesel	1 ↑	-
[77]	CR of 18 in CDC mode at 4.5 bar with 1800 rpm	Diesel + jatropa + heptanol (40 + 20 + 40)	38	5 ↓	-	14 ↑	41.6 ↓
[78]	CR of 17.5 in CDC mode at 6 bar with 1500 rpm	Diesel + calophyllum inophyllum Decanol (50 + 10 + 40)	34.5	0.15 ↓	Slight increase in cylinder peak pressure compared to diesel	35 ↑	44 ↓
[79]	CR of 16.1 RCCI at 4 bar with 1300 rpm	LRF-methane/HR F-diesel, PR-85	50.7 GIE	3.37 ↑	Advancement of peak pressure occurs at RCCI mode.	97	98 ↓
[80]	CR 16.8 of RCCI at 5 bar with 1200 rpm, EGR-12.5-26	Fuel-LR-ethanol/HR-diesel	46	2 ↓	CDC mode has higher ROHR compared to RCCI mode.	88 ↓	55 ↓
[81]	CR 14.9 of RCCI at 6.5 bar with 1300 rpm, EGR-42	LRF-E85 + EHN3/HRF-diesel	59.1 GIE	-	-	-	-
[17]	CR of 16.1 RCCI at 9.3 bar with 1300 rpm, EGR-41,	LRF-gasoline/HR F-diesel, PR-89	56.1 GIE	14 ↑	Increased PRRR (49%) and ROHR compared to CDC mode of operation	99 ↓	84 ↓
[82]	CR of 16 RCCI at 10 bar with 1500 rpm, EGR-0-50	LRF-butanol/HR F-biodiesel, PR-20-80	48.5	4 ↑	For maximum premixing Ratio leads to maximum peak pressure and ROHR.	38 ↓	2 ↑
[83]	CR 16 of RCCI at 9.2 bar with 2000 rpm, EGR-0-50	LRF-ethanol/HR F-diesel, PR-55-87	46.5	2 ↑	Increased ROHR with increased injection pressure	-	59 ↓

A-BTE—absolute brake thermal efficiency, D-BTE-difference in brake thermal efficiency, ↑ Increases, ↓ Decreases. GIE-gross indicate d efficiency, For CDC, % change is with reference to diesel fuel, for RCCI, % changes are with respect to changes in PR.

Intake air temperature is another parameter that significantly influences the rate of pressure rise. This is because the combustion in RCCI is dominated by chemical effects and temperature can affect ignition dynamics. When the engine is equipped with a turbocharger and EGR, multiple combinations of intake temperature can be achieved. The effect of intake temperature on the RCCI operation under such conditions is not yet explored thoroughly. Dual-peak heat release curves showed improved engine performance and lower emissions in the CDC operation [84]. In-cylinder combustion of RCCI can be optimized by injection strategies to obtain dual-peak heat release curves. Such combustion optimization can yield further improvements to RCCI engines. In addition to reducing the heat losses during the combustion, piston bowl shapes can further be optimized to improve mixing between the HRF and air + LRF mixture. HRF injector configurations in terms of the number of holes, injection pressure, pulse rate, and duration can be optimized together with the piston bowl shape. Such optimization can reduce soot, HC, and CO emissions similar to those observed for CDC engines. Established technologies of CDC such as variable valve timings, internal EGR, and multistage turbocharging can be extended to the RCCI operation. A lower compression ratio of 11 can be used for the RCCI operation as it has the potential for high-load operation. However, reduction in performance at low and medium loads can be nullified with the above-said established CDC technologies. Even with a compression ratio of 11, EGR is used to achieve high loads. There is a need to reduce the EGR rate as, fundamentally, the RCCI concept was developed to avoid EGR. Cooling the EGR can reduce the intake temperature and lower the rate of pressure rise also. Hence, EGR coolers can be used to reduce EGR rates, which reduces HC/CO emissions and increase combustion efficiency. The majority of high load operation with the RCCI engine was achieved with diesel as HRF. Hence investigations can be performed with biodiesels at high-load operation.

The accuracy of computational modeling of RCCI combustion needs to be improved. As discussed earlier, significant differences between CFD-predicted and measured HRR of RCCI operation at high load points are observed. As chemical kinetics dominates RCCI combustion, models that describe ignition dynamics, intermediate chemical reactions, and multicomponent diffusion need to be thoroughly analyzed and validated with suitable experimental data. With many control parameters, choosing the optimum-configuration RCCI engine is a very complicated task. Hence, one-dimensional thermodynamic tools with proper validation can be used to reduce engine testing. Estimation of RCCI engine performance with various premixing ratios, EGR rate, compression ratio, etc., can be performed with a one-dimensional tool. Optimization algorithms, which are based on artificial neural networks [85,86], and genetic algorithms [41] can be used to optimize injection strategies.

The main advantage of RCCI engines is that aftertreatment devices such as DPF and SCR are not required. Further, RCCI enhances thermal efficiency by about 5–10% compared to CDC. RCCI engines have certain limitations also. As the combustion temperatures are lowered, HC and CO emissions increase, as shown in Tables 1–6. Hence, a diesel oxidation catalyst should be used to reduce these emissions. Another limitation of RCCI is high load operation. When the load is increased beyond 13 bar IMEP, excessive pressure rise can be observed. This leads to higher amounts of NO<sub>x</sub>. To reduce the rate of pressure rise, various techniques such as EGR, compression ratio, and injection strategy are used. A brief discussion of these solutions is explained in Section 3. Further, at high loads, PR is higher and so the power cycle approaches homogeneous combustion. This can result in knocking. Algorithms to detect and control knocking for the RCCI operation need to be developed.

The main obstacle to implementing RCCI technology in production engines is high-load operation. For loads below 10 bar, the rate of pressure rise is within acceptable limits. The BMEP of an engine generating 16 hp at 3600 rpm with 625 cm<sup>3</sup> swept volume is 6.36 bar. Some of the light commercial vehicles use engines of this performance. Hence, RCCI can be implemented for LCVs. A rigorous study of RCCI combustion at speeds in the range of 3000–4000 RPM needs to be investigated for this purpose. The emission

testing cycle will consist of vehicle acceleration and deceleration. The response of RCCI combustion to such transient conditions should be investigated. Generators with a power capacity of less than 15 kW can be another application for RCCI. The fixed-speed operation of generators will offer some flexibility in optimizing the engine hardware for thermal efficiency and RCCI combustion control strategy.

In the transport sector, the market for EVs is progressively increasing. This growth rate is contributed to by government policies and customer preferences. When EVs are charged with renewable energy sources, they provide net-zero emissions. However, the infrastructure in the renewable energy sector is not good enough to provide power for all EVs [87]. So, a significant amount of EVs will be charged by conventional power stations, which use coal- or hydrocarbon-based fuels. This nullifies the leverage of EV vehicles toward net-zero emissions. If one accounts for the transmission losses from the power source to charging stations, then net emissions produced by EVs are comparable to those of ICE vehicles. Further, the manufacturing of batteries requires huge amounts of rare-earth elements, whose mining is a power-consuming activity [88]. The disposal of batteries is also a concern, as they pollute land [89,90]. Hence, life-cycle emissions of EVs are comparable to those of ICE vehicles even when they are charged with renewable sources. In summary, EVs may provide net-zero tailpipe emissions, but from the perspective of life-cycle and battery disposal, they are not zero-emission vehicles. There is a need to spread this awareness to policymakers, government regulating bodies, and the common public.

The present battery technology is not good enough for EVs to replace the ICE vehicles in the commercial vehicle segments [87,91]. Hence, ICE vehicles are going to dominate in commercial segments for the next few decades. Similarly, ships, generators, and heavy equipment will be powered by ICEs for several decades. This indicates that ICEs have a bright future for the next few decades, and government regulating bodies and policymakers should not abruptly prefer other technologies. Hence, a thorough analysis of life-cycle emissions should be made for each application and technology, and then policies should be framed with the aim of reducing emissions, thus paving the way for a cleaner environment.

It may take nearly 2–3 decades to furnish the necessary infrastructure in the renewable energy sector to provide sufficient power for charging all EV vehicles. Until then, EVs cannot be treated as net-zero emission vehicles. During this transition period, the transport sector will be dominated by ICE vehicles, and so the environment will continue to receive CO<sub>2</sub> and other exhaust emissions. The 2017 data of Ritchie and Roser [92] indicate that the transport sector contributes to 10% of global CO<sub>2</sub> emissions. So, there is a greater responsibility on IC engine designers to make it more fuel efficient, thereby reducing CO<sub>2</sub> emissions. The thermal efficiency of the vehicle can be improved by switching to a diesel cycle from the gasoline cycle, weight reduction, effective thermal management (including at start and idling conditions), and LTC concepts such as RCCI, mechanical friction reduction, and effective utilization of exhaust energy. As shown in Table 7, biodiesel blends lead to higher fuel consumption. Mostly biodiesels are made from local resources, and CO<sub>2</sub> emissions released for generating biofuels can be significantly lower compared to those for hydrocarbon-based fuels. A majority of hydrocarbon fuels are extracted, refined, and processed in Middle Eastern countries, and fuel is transported to other continents. The burden of this transport is taken again by ICE-based ships/vehicles. So, when one accounts for CO<sub>2</sub> emissions from source to end-use, it is found that biofuels emit less CO<sub>2</sub> into the atmosphere. This gives a boost to the local economy also, providing a way for a sustainable society. Hence, policymakers and engine-makers should push for higher blends of bio-derived fuels [93–95].

#### 4. Conclusions

RCCI engine is a dual fuel operation, where low reactive fuel will be injected in the intake port and high reactive fuel will be injected into the cylinder. The paper reviews recent investigations on RCCI engines, and emission data presented in the article demonstrates the capability to achieve Euro 6 emission norms without aftertreatment devices for NO<sub>x</sub>

and soot. Effects of various engine operating parameters such as type of fuels, premixing ratio, EGR rate and compression ratio are discussed. Heat transfer losses, HC and CO emissions obtained on different piston bowl shapes are delineated. The methods used to extend the operating range of the RCCI concept to high loads are explained.

When the premixing ratio is increased ignition delay is increased, and hence relatively higher time is available for mixing between high reactivity fuel and air. Physical properties of low and high-reactive fuels also influence the ignition delay. An increase in ignition delay helps in reducing the NO<sub>x</sub> and soot simultaneously. Various fuels such as gasoline, iso-propanol, iso-butanol, methanol, ethanol, 2,5-dimethylfuran, n-amyl alcohol, CNG+H<sub>2</sub> mixture, methane and natural gas, etc., are attempted as low reactivity fuels. Diesel, PODE, bio-diesel, etc., are used as high-reactive fuels. Depending on the load, pre-mixing ratios ranged from 30% to 85%. EGR in the RCCI engine is used to control the rate of pressure rise. Due to its higher heat capacity, EGR also results in a decrease in engine-out NO<sub>x</sub>. The attempted EGR ratios are in the range of 15% to 50%. As a penalty with EGR, thermal efficiency decreases, and HC and CO emissions increase. A lower compression ratio is preferred to have a lower rate of pressure rise and NO<sub>x</sub> emissions. The majority of RCCI operations are performed with compression ratios ranging from 14 to 17. The minimum attempted compression ratio is 11. Piston bowl shapes with stock, step, and bathtub are tested at low, medium and high load points. The stock-shaped piston bowl was found to be more suitable for RCCI operation. Computational fluid dynamics simulations revealed that the shape of the bowl has a lot of impact on heat transfer losses and HC and CO emissions. Piston bowl depth and squish region are optimized to reduce HC, CO emissions and heat transfer losses. By optimizing injection strategies, compression ratio, EGR rate and piston bowl shape high load operation on RCCI engines can be achieved. Engine load as high as 23 bar BMEP is achieved with a combination of late single injection strategy compression ratio: 11, pre-mixing ratio: 53, EGR rate: 36% and stock piston bowl.

Electric vehicles cannot be treated as zero-emission vehicles if they are not charged with renewable sources. This fact needs to be popularized among the common public and policymakers. Until alternative and affordable power sources are available, the transport sector will be powered by IC engines, and they continue to pollute the environment. By designing more efficient engines, the extent of pollution can be reduced. In compression ignition mode, diesel can be substituted with blends of biodiesel. On a fuel-to-fuel basis, biodiesel can lead to higher CO<sub>2</sub> emissions, but when life-cycle emissions are accounted for, biodiesel emits a lesser amount of CO<sub>2</sub>. Further usage of biodiesel blends reduces HC and CO emissions. Switching to the RCCI operation can increase thermal efficiency by about 10% with a corresponding reduction in CO<sub>2</sub> emissions. Future research in RCCI engines can be aimed at understanding RCCI behavior in acceleration and decelerations. Further investigations should be performed to study RCCI combustion for speeds in the range of 3000–4000 rpm. The performance, efficiency, and emissions from the RCCI engine can further be optimized with a combination of hydrogen mixtures as LRF, biodiesel as HRF, lower EGR rates, piston bowl shapes, injection strategies, and cold EGR. Efficiency improvements with dual-peak heat release curves, variable valve timings, higher swirl ratios, and mechanical friction reduction techniques should be explored. Studies should be performed to enhance the understanding of diffusion between LRF, HRF and air during the compression and combustion phase. Such diffusion is a key factor which results in fuel stratification. Hence efforts should be directed towards the right combination of fuels for LRF and HRF which can provide a simultaneous reduction in NO<sub>x</sub> and soot. There is a need to design IC engines on an application-to-application basis with the objective of reducing CO<sub>2</sub>, soot, and NO<sub>x</sub> emissions simultaneously. From this perspective, RCCI should be implemented in light commercial vehicles and generators whose power rating is below 16 hp.

**Author Contributions:** Conceptualization, methodology, validation, resources, writing (original draft), writing (review and editing), project administration, S.K.R.D.; investigation, validation, resources, post-processing of data, writing (original draft); S.S.R.; writing (review and editing), O.R.K.; review and proofread, E.P.V.; review and editing, I.V.; Editing and revising, O.D.S.; All authors have read and agreed to the published version of the manuscript.

**Funding:** This research received no external funding.

**Data Availability Statement:** Not applicable.

**Conflicts of Interest:** The authors declare no conflict of interest.

## Abbreviations

BMEP	Brake mean effective pressure
BSFC	Brake-specific fuel consumption
CA	Crank angle
CDC	Conventional diesel combustion
CH <sub>3</sub> OH	Methanol
CI	Compression ignition
CNG	Compressed natural gas
CO	Carbon monoxide
CO <sub>2</sub>	Carbon dioxide
CR	Compression ratio
DI	Direct injection
EGR	Exhaust gas recirculation
HC	Hydrocarbon
HCCI	Homogeneous charge compression Ignition
HRR	Heat release rate
HRF	High-reactivity fuel
HTHR	High-temperature heat release
ID	Ignition delay
IVC	Inlet valve closing
LRF	Low-reactivity fuel
LTC	Low-temperature combustion
LTHR	Low-temperature heat release
NO <sub>x</sub>	Nitrogen oxide
NTC	Negative-temperature coefficient
PCCI	Premixed charge compression ignition
PFI	Port fuel injection
PODE	Polyoxy methylene dimethyl ethers
PR	Premixing ratio
RPM	Revolution per minute
RCCI	Reactivity-controlled compression ignition
SI	Spark ignition
SOC	Start of combustion
SOI	Start of injection
TDC	Top dead center

## References

1. Prasad, R.; Bella, V.R. A review on diesel soot emission, its effect and control. *Bull. Chem. React. Eng. Catal.* **2010**, *5*, 69. [CrossRef]
2. Bhandarkar, S. Vehicular pollution, their effect on human health and mitigation measures. *Veh. Eng.* **2013**, *1*, 33–40.
3. Reitz, R.D. Directions in internal combustion engine research. *Combust. Flame* **2013**, *160*, 1–8. [CrossRef]
4. Lindqvist, K. Emission standards for light and heavy road vehicles. AirClim Factsheet 2012, Volume 25. Available online: <https://www.airclim.org/sites/default/files/documents/Factsheet-emission-standards.pdf> (accessed on 16 January 2023).
5. Zimmermann, K.; Haefeli, R.; Ganser, M. Engine performances with advanced common rail injector Design. In Proceedings of the ASME 2017 Internal Combustion Engine Division Fall Technical Conference, Washington, DC, USA, 15–18 October 2017; American Society of Mechanical Engineers: New York, NY, USA, 2017; p. 58318. [CrossRef]

6. Yu, R.C.; Shahed, S.M. Effects of injection timing and exhaust gas recirculation on emissions from a DI diesel engine. *SAE Trans.* **1981**, *90*, 3873–3883. [[CrossRef](#)]
7. Brandi, F.K.; Affenzeller, J.; Thien, G.E. Some strategies to meet future noise regulations for truck engines. *SAE Trans.* **1987**, *96*, 1510–1521. [[CrossRef](#)]
8. Reddy, D.S.K.; Ghodke, P.; Velusamy, R. Indigenous Knowledge Generation in the Design of Automotive Engines. In Proceedings of the India International Science Festival, Department of Science and Technology, Government of India, New Delhi, India, 4–8 December 2015. Paper No. 120.
9. Shaik, R.; Kumar, A.; Padmavathi, R.; Jagan, G.; Anshul, A.; Ganguly, G.; Dwarshala, K.; Ravishankar, S.S. *Computational and Experimental Investigations to Improve Performance, Emissions and Fuel Efficiency of a Single Cylinder Diesel Engine*; SAE Technical Paper; SAE: Warrendale, PA, USA, 2015; Paper No. 99.
10. Jackson, M.W. Effect of catalytic emission control on exhaust hydrocarbon composition and reactivity. *SAE Trans.* **1978**, *87*, 2304–2327.
11. Abthoff, J.; Schuster, H.D.; Langer, H.J.; Loose, G. The Regenerable Trap Oxidizer—An Emission Control Technique for Diesel Engines. *SAE Trans.* **1985**, *94*, 128–138. [[CrossRef](#)]
12. Kummer, J.T. Catalysts for automobile emission control. *Prog. Energy Combust. Sci.* **1980**, *6*, 177–199. [[CrossRef](#)]
13. Wilson, D.E. The design of a low specific fuel consumption turbocompound engine. *SAE Trans.* **1986**, *1*, 445–459. [[CrossRef](#)]
14. Heywood, J.B. *Internal Combustion Engine Fundamentals*; McGraw-Hill Education: New York, NY, USA, 2018.
15. Pachiannan, T.; Zhong, W.; Rajkumar, S.; He, Z.; Leng, X.; Wang, Q. A literature review of fuel effects on performance and emission characteristics of low-temperature combustion strategies. *Appl. Energy* **2019**, *251*, 113380. [[CrossRef](#)]
16. Jain, A.; Singh, A.P.; Agarwal, A.K. Effect of split fuel injection and EGR on NO<sub>x</sub> and PM emission reduction in a low temperature combustion (LTC) mode diesel engine. *Energy* **2017**, *122*, 249–264. [[CrossRef](#)]
17. Kokjohn, S.L.; Hanson, R.M.; Splitter, D.A.; Reitz, R.D. Fuel reactivity-controlled compression ignition (RCCI): A pathway to controlled high-efficiency clean combustion. *Int. J. Engine Res.* **2011**, *12*, 209–226. [[CrossRef](#)]
18. Ministry of Petroleum; Natural Gas; Government of India. 1 September 2022. Available online: <https://ppac.gov.in/> (accessed on 16 January 2023).
19. El-Emam, S.H.; Desoky, A.A. A study on the combustion of alternative fuels in spark-ignition engines. *Int. J. Hydrogen Energy* **1985**, *10*, 497–504. [[CrossRef](#)]
20. Gabele, P.A.; Baugh, J.O.; Black, F.; Snow, R. Characterization of emissions from vehicles using methanol and methanol-gasoline blended fuels. *J. Air Pollut. Control. Assoc.* **1985**, *35*, 1168–1175. [[CrossRef](#)]
21. De Carvalho, A.V., Jr. Natural gas and other alternative fuels for transportation purposes. *Energy* **1985**, *10*, 187–215. [[CrossRef](#)]
22. Napolitano, P.; Guido, C.; Beatrice, C.; Di Blasio, G. Study of the effect of the engine parameters calibration to optimize the use of bio-ethanol/RME/diesel blend in a Euro5 light duty diesel engine. *SAE Int. J. Fuels Lubr.* **2013**, *6*, 263–275. [[CrossRef](#)]
23. Murray, R.; Wyse-Mason, R. Investigation of methanol-biodiesel-coconut oil ternary blends as an alternative fuel for CI engines. *Eng. Sci. Technol. Int. J.* **2018**, *21*, 1056–1066. [[CrossRef](#)]
24. Zhang, Z.H.; Balasubramanian, R. Influence of butanol addition to diesel–biodiesel blend on engine performance and particulate emissions of a stationary diesel engine. *Appl. Energy* **2014**, *119*, 530–536. [[CrossRef](#)]
25. Banapurmath, N.R.; Tewari, P.G.; Yaliwal, V.S.; Kambalimath, S.; Basavarajappa, Y.H. Combustion characteristics of a 4-stroke CI engine operated on Honge oil, Neem and Rice Bran oils when directly injected and dual fuelled with producer gas induction. *Renew. Energy* **2009**, *34*, 1877–1884. [[CrossRef](#)]
26. Plotnikov, L.V.; Ulman, N.V. Computational and analytical evaluation of the efficiency of using hydrogen as a fuel in an internal combustion engine. *IOP Conf. Ser. Earth Environ. Sci.* **2021**, *723*, 052018. [[CrossRef](#)]
27. Maurya, R.K.; Agarwal, A.K. Experimental study of combustion and emission characteristics of ethanol fuelled port injected homogeneous charge compression ignition (HCCI) combustion engine. *Appl. Energy* **2011**, *88*, 1169–1180. [[CrossRef](#)]
28. Inagaki, K.; Fuyuto, T.; Nishikawa, K.; Nakakita, K.; Sakata, I. *Dual-Fuel PCI Combustion Controlled by in-Cylinder Stratification of Ignitability*; SAE Technical Paper; SAE: Warrendale, PA, USA, 2006.
29. Splitter, D.; Hanson, R.; Kokjohn, S.; Reitz, R.D. *Reactivity Controlled Compression Ignition (RCCI) Heavy-Duty Engine Operation at Mid-and High-Loads with Conventional and Alternative Fuels*; SAE Technical Paper; SAE: Warrendale, PA, USA, 2011. [[CrossRef](#)]
30. Agarwal, A.K.; Singh, A.P.; Maurya, R.K. Evolution, challenges and path forward for low temperature combustion engines. *Prog. Energy Combust. Sci.* **2017**, *61*, 1–56. [[CrossRef](#)]
31. Tompkins, B.T.; Jacobs, T.J. Low-temperature combustion with biodiesel: Its enabling features in improving efficiency and emissions. *Energy Fuels* **2013**, *27*, 2794–2803. [[CrossRef](#)]
32. Bergthorson, J.M.; Thomson, M.J. A review of the combustion and emissions properties of advanced transportation biofuels and their impact on existing and future engines. *Renew. Sustain. Energy Rev.* **2015**, *42*, 1393–1417. [[CrossRef](#)]
33. Thangaraja, J.; Kannan, C. Effect of exhaust gas recirculation on advanced diesel combustion and alternate fuels—A review. *Appl. Energy* **2016**, *180*, 169–184. [[CrossRef](#)]
34. Jiaqiang, E.; Pham, M.; Zhao, D.; Deng, Y.; Le, D.; Zuo, W.; Zhu, H.; Liu, T.; Peng, Q.; Zhang, Z. Effect of different technologies on combustion and emissions of the diesel engine fueled with biodiesel: A review. *Renew. Sustain. Energy Rev.* **2017**, *80*, 620–647. [[CrossRef](#)]
35. Ganesan, V. *Internal Combustion Engines*, 3rd ed.; McGraw Hill Education (India) Pvt Ltd.: New York, NY, USA, 2012.

36. Dec, J.E. A conceptual model of DL diesel combustion based on laser-sheet imaging. *SAE Trans.* **1997**, *106*, 1319–1348. [[CrossRef](#)]
37. Reddy, D.S.K.; Kumar, P. Application of CFD in the Design of Reciprocating Engine for Light Commercial Vehicle Applications. In *Alternative Fuels and Advanced Combustion Techniques as Sustainable Solutions for Internal Combustion Engines*; Springer: Singapore, 2021; pp. 347–375. [[CrossRef](#)]
38. Wissink, M.L. Direct Injection for Dual Fuel Stratification: Improving the Control of Heat Release in Advanced IC Engine Combustion Strategies. Ph.D. Thesis, University of Wisconsin-Madison, Madison, WI, USA, 2015.
39. Olmeda, P.; Garcia, A.; Monsalve-Serrano, J.; Sari, R.L. Experimental investigation on RCCI heat transfer in a light-duty diesel engine with different fuels: Comparison versus conventional diesel combustion. *Appl. Therm. Eng.* **2018**, *144*, 424–436. [[CrossRef](#)]
40. Murugan, R.; Ganesh, D.; Nagarajan, G. An integrated effort of medium reactivity fuel, in-cylinder, and after-treatment strategies to demonstrate potential reduction in challenging emissions of reactivity-controlled compression ignition combustion. *Proc. Inst. Mech. Eng. Part D J. Automob. Eng.* **2020**, *234*, 1260–1278. [[CrossRef](#)]
41. Nieman, D.E.; Dempsey, A.B.; Reitz, R.D. Heavy-duty RCCI operation using natural gas and diesel. *SAE Int. J. Engines* **2012**, *5*, 270–285. [[CrossRef](#)]
42. Qian, Y.; Ouyang, L.; Wang, X.; Zhu, L.; Lu, X. Experimental studies on combustion and emissions of RCCI fueled with n-heptane/alcohols fuels. *Fuel* **2015**, *162*, 239–250. [[CrossRef](#)]
43. Jo, S.; Park, S.; Kim, H.J.; Lee, J.T. Combustion improvement and emission reduction through control of ethanol ratio and intake air temperature in reactivity controlled compression ignition combustion engine. *Appl. Energy* **2019**, *250*, 1418–1431. [[CrossRef](#)]
44. Okcu, M.; Varol, Y.; Altun, Ş.; Firat, M. Effects of isopropanol-butanol-ethanol (IBE) on combustion characteristics of a RCCI engine fueled by biodiesel fuel. *Sustain. Energy Technol. Assess.* **2021**, *47*, 101443. [[CrossRef](#)]
45. Ghaffarzadeh, S.; Toosi, A.N.; Hosseini, V. An experimental study on low temperature combustion in a light duty engine fueled with diesel/CNG and biodiesel/CNG. *Fuel* **2020**, *262*, 116495. [[CrossRef](#)]
46. Ganesh, D.; Ayyappan, P.R.; Murugan, R. Experimental investigation of isobutanol /diesel reactivity-controlled compression ignition combustion in a non-road diesel engine. *Appl. Energy* **2019**, *242*, 1307–1319. [[CrossRef](#)]
47. Duraisamy, G.; Rangasamy, M.; Govindan, N.A. comparative study on methanol/diesel and methanol/PODE dual fuel RCCI combustion in an automotive diesel engine. *Renew. Energy* **2020**, *145*, 542–556. [[CrossRef](#)]
48. Pan, S.; Liu, X.; Cai, K.; Li, X.; Han, W.; Li, B. Experimental study on combustion and emission characteristics of iso-butanol/diesel and gasoline/diesel RCCI in a heavy-duty engine under low loads. *Fuel* **2020**, *261*, 116434. [[CrossRef](#)]
49. Harari, P.A.; Banapurmath, N.R.; Yaliwal, V.S.; Khan, T.Y.; Soudagar, M.E.M.; Sajjan, A.M. Experimental studies on performance and emission characteristics of reactivity-controlled compression ignition (RCCI) engine operated with gasoline and Thevetia Peruviana biodiesel. *Renew. Energy* **2020**, *160*, 865–875. [[CrossRef](#)]
50. Liu, H.; Ma, G.; Hu, B.; Zheng, Z.; Yao, M. Effects of port injection of hydrous ethanol on combustion and emission characteristics in dual-fuel reactivity-controlled compression ignition (RCCI) mode. *Energy* **2018**, *145*, 592–602. [[CrossRef](#)]
51. Biswas, S.; Kakati, D.; Chakraborti, P.; Banerjee, R. Assessing the potential of ethanol in the transition of biodiesel combustion to RCCI regimes under varying injection phasing strategies: A performance-emission-stability and tribological perspective. *Fuel* **2021**, *304*, 121346. [[CrossRef](#)]
52. Isik, M.Z.; Aydın, H. Analysis of ethanol RCCI application with safflower biodiesel blends in a high load diesel power generator. *Fuel* **2016**, *184*, 248–260. [[CrossRef](#)]
53. Wang, H.; Tong, L.; Zheng, Z.; Yao, M. Experimental study on high-load extension of gasoline/PODE dual-fuel RCCI operation using late intake valve closing. *SAE Int. J. Engines* **2017**, *10*, 1482–1490. [[CrossRef](#)]
54. Zhao, W.; Zhang, Y.; Huang, G.; He, Z.; Qian, Y.; Lu, X. Experimental investigation on combustion and emission characteristics of butanol/biodiesel under blend fuel mode, dual fuel RCCI and ICCI modes. *Fuel* **2021**, *305*, 121590. [[CrossRef](#)]
55. Baskovic, U.Z.; Opresnik, S.R.; Seljak, T.; Katrasnik, T. RCCI combustion with renewable fuel mix—Tailoring operating parameters to minimize exhaust emissions. *Fuel* **2022**, *311*, 122590. [[CrossRef](#)]
56. Duraisamy, G.; Rangasamy, M.; Nagarajan, G. *Effect of EGR and Premixed Mass Percentage on Cycle to Cycle Variation of Methanol/Diesel Dual Fuel RCCI Combustion*; SAE Technical Paper; SAE: Warrendale, PA, USA, 2019; Volume 26, p. 260090. [[CrossRef](#)]
57. Motallebi Hasankola, S.S.; Shafaghat, R.; Jahanian, O.; TaleshAmiri, S.; Shooghi, M. Numerical investigation of the effects of inlet valve closing temperature and exhaust gas recirculation on the performance and emissions of an RCCI engine. *J. Therm. Anal. Calorim.* **2020**, *139*, 2465–2474. [[CrossRef](#)]
58. Khatamnejad, H.; Khalilarya, S.H.; Jafarmadar, S.; Mirsalim, M. The effect of high-reactivity fuel injection parameters on combustion features and exhaust emission characteristics in a natural gas–diesel RCCI engine at part load condition. *Int. J. Green Energy* **2018**, *15*, 874–888. [[CrossRef](#)]
59. Benajes, J.; Molina, S.; García, A.; Monsalve-Serrano, J. Effects of low reactivity fuel characteristics and blending ratio on low load RCCI (reactivity controlled compression ignition) performance and emissions in a heavy-duty diesel engine. *Energy* **2015**, *90*, 1261–1271. [[CrossRef](#)]
60. Poorghasemi, K.; Saray, R.K.; Ansari, E.; Irdmousa, B.K.; Shahbakhti, M.; Naber, J.D. Effect of diesel injection strategies on natural gas/diesel RCCI combustion characteristics in a light duty diesel engine. *Appl. Energy* **2017**, *199*, 430–446. [[CrossRef](#)]
61. Kakaee, A.H.; Nasiri-Toosi, A.; Partovi, B.; Paykani, A. Effects of piston bowl geometry on combustion and emissions characteristics of a natural gas/diesel RCCI engine. *Appl. Therm. Eng.* **2016**, *102*, 1462–1472. [[CrossRef](#)]

62. Jia, Z.; Denbratt, I. Experimental investigation of natural gas-diesel dual-fuel RCCI in a heavy-duty engine. *SAE Int. J. Engines* **2015**, *8*, 797–807. [[CrossRef](#)]
63. Xu, G.; Jia, M.; Li, Y.; Chang, Y.; Liu, H.; Wang, T. Evaluation of variable compression ratio (VCR) and variable valve timing (VVT) strategies in a heavy-duty diesel engine with reactivity controlled compression ignition (RCCI) combustion under a wide load range. *Fuel* **2019**, *253*, 114–128. [[CrossRef](#)]
64. Sharma, M.; Kaushal, R. Performance and exhaust emission analysis of a variable compression ratio (VCR) dual fuel CI engine fuelled with producer gas generated from pistachio shells. *Fuel* **2021**, *283*, 118924. [[CrossRef](#)]
65. Benajes, J.; Pastor, J.V.; García, A.; Monsalve-Serrano, J. An experimental investigation on the influence of piston bowl geometry on RCCI performance and emissions in a heavy-duty engine. *Energy Convers. Manag.* **2015**, *103*, 1019–1030. [[CrossRef](#)]
66. Dalha, I.B.; Said, M.A.; Karim, Z.A.A.; El Adawy, M. Effects of port mixing and high carbon dioxide contents on power generation and emission characteristics of biogas-diesel RCCI combustion. *Appl. Therm. Eng.* **2021**, *198*, 117449. [[CrossRef](#)]
67. Aydin, H. An innovative research on variable compression ratio in RCCI strategy on a power generator diesel engine using CNG-safflower biodiesel. *Energy* **2021**, *231*, 121002. [[CrossRef](#)]
68. Benajes, J.; García, A.; Pastor, J.M.; Monsalve-Serrano, J. Effects of piston bowl geometry on Reactivity Controlled Compression Ignition heat transfer and combustion losses at different engine loads. *Energy* **2016**, *98*, 64–77. [[CrossRef](#)]
69. Dempsey, A.B.; Curran, S.; Reitz, R.D. Characterization of reactivity controlled compression ignition (RCCI) using premixed gasoline and direct-injected gasoline with a cetane improver on a multi-cylinder engine. *SAE Int. J. Engines* **2015**, *8*, 859–877. [[CrossRef](#)]
70. Splitter, D.; Wissink, M.; Kokjohn, S.; Reitz, R.D. Effect of compression ratio and piston geometry on RCCI load limits and efficiency. *SAE World Congr. Exhib.* **2012**, *01*, 0383. [[CrossRef](#)]
71. Hanson, R.; Curran, S.; Wagner, R.; Kokjohn, S.; Splitter, D.; Reitz, R. Piston bowl optimization for RCCI combustion in a light-duty multi-cylinder engine. *SAE Int. J. Engines* **2012**, *5*, 286–299. [[CrossRef](#)]
72. Wategave, S.P.; Banapurmath, N.R.; Sawant, M.S.; Soudagar, M.E.M.; Mujtaba, M.A.; Afzal, A.; Sajjan, A.M. Clean combustion and emissions strategy using reactivity controlled compression ignition (RCCI) mode engine powered with CNG- Karanja biodiesel. *J. Taiwan Inst. Chem. Eng.* **2021**, *124*, 116–131. [[CrossRef](#)]
73. Wang, H.; Liu, D.; Ma, T.; Tong, L.; Zheng, Z.; Yao, M. Thermal efficiency improvement of PODE/Gasoline dual-fuel RCCI high load operation with EGR and air dilution. *Appl. Therm. Eng.* **2019**, *159*, 113763. [[CrossRef](#)]
74. Benajes, J.; García, A.; Monsalve-Serrano, J.; Boronat, V. Achieving clean and efficient engine operation up to full load by combining optimized RCCI and dual-fuel diesel-gasoline combustion strategies. *Energy Convers. Manag.* **2017**, *136*, 142–151. [[CrossRef](#)]
75. Dadsetan, M.; Chitsaz, I.; Amani, E. A study of swirl ratio effects on the NO<sub>x</sub> formation and mixture stratification in an RCCI engine. *Energy* **2019**, *182*, 1100–1114. [[CrossRef](#)]
76. Sathyamurthy, R.; Balaji, D.; Gorjian, S.; Muthiya, S.J.; Bharathwaaj, R.; Vasanthaseelan, S.; Essa, F.A. Performance, combustion and emission characteristics of a DI-CI diesel engine fueled with corn oil methyl ester biodiesel blends. *Sustain. Energy Technol. Assess.* **2021**, *43*, 100981. [[CrossRef](#)]
77. Kadian, A.K.; Khan, M.; Sharma, R.P. Performance enhancement and emissions mitigation of DI-CI engine fuelled with ternary blends of jatropha biodiesel-diesel-heptanol. *Mater. Sci. Energy Technol.* **2022**, *5*, 145–154. [[CrossRef](#)]
78. Nanthagopal, K.; Ashok, B.; Saravanan, B.; Pathy, M.R.; Sahil, G.; Ramesh, A.; Nabi, M.N.; Rasul, M.G. Study on decanol and Calophyllum Inophyllum biodiesel as ternary blends in CI engine. *Fuel* **2019**, *239*, 862–873. [[CrossRef](#)]
79. Rahnama, P.; Paykani, A.; Bordbar, V.; Reitz, R.D. A numerical study of the effects of reformer gas composition on the combustion and emission characteristics of a natural gas/diesel RCCI engine enriched with reformer gas. *Fuel* **2017**, *209*, 742–753. [[CrossRef](#)]
80. Pedrozo, V.B.; May, I.; Lanzanova, T.D.; Zhao, H. Potential of internal EGR and throttled operation for low load extension of ethanol–diesel dual-fuel reactivity controlled compression ignition combustion on a heavy-duty engine. *Fuel* **2016**, *179*, 391–405. [[CrossRef](#)]
81. Splitter, D.; Wissink, M.; DelVescovo, D.; Reitz, R.D. *RCCI Engine Operation towards 60% Thermal Efficiency*; SAE Technical Paper; SAE: Warrendale, PA, USA, 2013. [[CrossRef](#)]
82. Zheng, Z.; Xia, M.; Liu, H.; Shang, R.; Ma, G.; Yao, M. Experimental study on combustion and emissions of n-butanol/biodiesel under both blended fuel mode and dual fuel RCCI mode. *Fuel* **2018**, *226*, 240–251. [[CrossRef](#)]
83. Beatrice, C.; Denbratt, I.; Di Blasio, G.; Di Luca, G.; Ianniello, R.; Saccullo, M. Experimental assessment on exploiting low carbon ethanol fuel in a light-duty dual-fuel compression ignition engine. *Appl. Sci.* **2020**, *10*, 7182. [[CrossRef](#)]
84. Inaba, K.; Ojima, Y.; Masuko, Y.; Kobashi, Y.; Shibata, G.; Ogawa, H. Thermal efficiency improvement with super-charging and cooled exhaust gas recirculation in semi-premixed diesel combustion with a twin peak shaped heat release. *Int. J. Engine Res.* **2019**, *20*, 80–91. [[CrossRef](#)]
85. Okcu, M.; Firat, M.; Varol, Y.; Altun, Ş.; Kamsılı, F.; Atila, O. Combustion of high carbon (C7-C8) alcohol fuels in a reactivity controlled compression ignition (RCCI) engine as low reactivity fuels and ANN approach to predict RCCI emissions. *Fuel* **2022**, *319*, 123735. [[CrossRef](#)]
86. Koc, M.A.; Şener, R. Prediction of emission and performance characteristics of reactivity-controlled compression ignition engine with the intelligent software based on adaptive neural-fuzzy and neural-network. *J. Clean. Prod.* **2021**, *318*, 128642. [[CrossRef](#)]

87. Reitz, R.D.; Ogawa, H.; Payri, R.; Fansler, T.; Kokjohn, S.; Moriyoshi, Y.; Agarwal, A.K.; Arcoumanis, D.; Assanis, D.; Bae, C.; et al. IJER editorial: The future of the internal combustion engine. *Int. J. Engine Res.* **2020**, *21*, 3–10. [[CrossRef](#)]
88. Schreiber, A.; Marx, J.; Zapp, P.; Hake, J.F.; Voßenkaul, D.; Friedrich, B. Environmental impacts of rare earth mining and separation based on eudialyte: A new European way. *Resources* **2016**, *5*, 32. [[CrossRef](#)]
89. Makwarimba, C.P.; Tang, M.; Peng, Y.; Lu, S.; Zheng, L.; Zhao, Z.; Zhen, A.G. Assessment of recycling methods and processes for lithium-ion batteries. *Iscience* **2022**, *25*, 104321. [[CrossRef](#)]
90. Rajesh, R.; Kanakadhurga, D.; Prabakaran, N. Electronic waste: A critical assessment on the unimaginable growing pollutant, legislations and environmental impacts. *Environ. Chall.* **2022**, *7*, 100507. [[CrossRef](#)]
91. Goel, S.; Sharma, R.; Rathore, A.K. A review on barrier and challenges of electric vehicle in India and vehicle to grid optimisation. *Transp. Eng.* **2021**, *4*, 100057. [[CrossRef](#)]
92. Ritchie, H.; Roser, M.; Rosado, P. CO<sub>2</sub> and greenhouse gas emissions. Our World in Data. 2020. Available online: [https://ourworldindata.org/co2-emissions?utm\\_source=tri-city%20news&utm\\_campaign=tricity%20news%3A%20outbound&utm\\_medium=referral](https://ourworldindata.org/co2-emissions?utm_source=tri-city%20news&utm_campaign=tricity%20news%3A%20outbound&utm_medium=referral) (accessed on 16 January 2023).
93. Elumalai, P.V.; Pradeepkumar, A.R.; Murugan, M.; Saravanan, A.; Reddy, M.S.; Sree, S.R.; Sundaram, G.M. Analysis of performance, combustion, and emission parameters in a reactivity-controlled combustion ignition (RCCI) engine—an intensive review. *Int. J. Ambient. Energy* **2022**, *43*, 6839–6848. [[CrossRef](#)]
94. Murugesan, P.; Hoang, A.T.; Venkatesan, E.P.; Kumar, D.S.; Balasubramanian, D.; Le, A.T. Role of hydrogen in improving performance and emission characteristics of homogeneous charge compression ignition engine fueled with graphite oxide nanoparticle-added. *Int. J. Hydrogen Energy* **2021**, *47*, 37617–37634. [[CrossRef](#)]
95. Parthasarathy, M.; Ramkumar, S.; Isaac JoshuaRamesh Lalvani, J.; Elumalai, P.V.; Dhinesh, B.; Krishnamoorthy, R.; Thiyagarajan, S. Performance analysis of HCCI engine powered by tamanu methyl ester with various inlet air temperature and exhaust gas recirculation ratios. *Fuel* **2020**, *282*, 118833. [[CrossRef](#)]

**Disclaimer/Publisher’s Note:** The statements, opinions and data contained in all publications are solely those of the individual author(s) and contributor(s) and not of MDPI and/or the editor(s). MDPI and/or the editor(s) disclaim responsibility for any injury to people or property resulting from any ideas, methods, instructions or products referred to in the content.